# The three-dimensional (3D) organization of telomeres during cellular transformation

**By**

**Tony Chih-Yuan Chuang, M.D.**

**A Thesis submitted to the Faculty of Graduate Studies of**

**The University of Manitoba**

**in partial fulfilment of the requirements of the degree of**

**MASTER OF SCIENCE**

**Department of Physiology**

**University of Manitoba**

**Winnipeg, Manitoba, Canada**

## Abstract

### Statement of Problem

Telomere dynamics in the three-dimensional (3D) space of the mammalian nucleus plays an important role in the maintenance of genomic stability. However, the telomere distribution in 3D nuclear space of normal and tumor cells was unknown when the study was initiated.

### Methods

Telomere fluorescence *in situ* hybridization (FISH) and 3D molecular imaging, deconvolution, and analysis were used to investigate telomere organization in normal, immortalized and tumor cells from mouse and human cell lines, and primary tissues.

### Results

Telomeres are organized in a non-overlapping manner and in a cell-cycle dependant fashion in normal cells. In the late G2 phase of cell cycle, telomeres are assembled into a flattened sphere that is termed the telomeric disk In contrast, the telomeric disk is disrupted in the tumor cells. Moreover, telomeric aggregates (TAs) are found in tumor cells. Conditional *c-Myc* over-expression induces telomeric aggregation leading to the onset of breakage-bridge-fusion cycles and subsequent chromosomal abnormality.

### Conclusions

Telomeres are distributed in a nonrandom and dynamic fashion in the 3D space of a normal cell. Telomeric aggregates are present in cells with genomic instability such as tumor cells and cells with deregulation of *c-Myc*. Consequently, TA can be a useful biomarker for research in cancer and other disease processes.

## Acknowledgements

First of all, I want to thank my family for standing behind me without failing during the great turbulences I endured in my pursuit of my training and research.

"If I have seen further it is only by standing on the shoulders of giants." Sir Isaac Newton, in letter to Robert Hooke.

The work done in my thesis is made possible due to the collaboration with many giants, from different scientific disciplines and different parts of the world, with the same spirit of answering fundamental questions of any novel scientific observation – "what is it" and "why is it".

Much gratitude goes to my supervisor and committee members, Drs. Sabine Mai, Paul Kerr, James Davie, Robert Shiu, and Edwin Kroeger. You have given me different sets of skills, from critical thinking to performing head and neck surgery, that will be forever treasured by me.

Support from the Department of Physiology is much appreciated. Gail, I thank you for all your time and encouragement in getting me to completion of my study.

The financial support of this project was provided by the CIHR Strategic Training Program Grant to SM for "Innovative Technologies In Multidisciplinary Health Research Training Program" (www.itmhrt.ca).

## Dedication

To members of my family, friends and mentors from various institutions including University of Manitoba, The Johns Hopkins University, National Institutes of Health, and Delft University.

## Lists of Tables and Figures

List of tables – see publications Chuang et al, 2004 and Louis et al, 2005

List of figures – see publications Chuang et al, 2004 and Louis et al, 2005

Chuang, T.C., Moshir, S., Garini, Y., Chuang, A.Y., Young, I.T., Vermolen, B., van den Doel, R., Mougey, V., Perrin, M., Braun, M., et al. (2004). *The three-dimensional organization of telomeres in the nucleus of mammalian cell.* BMC Biol 2, 12.

Louis, S.F., Vermolen, B.J., Garini Y., Young, I.T., Guffei, A., Lichtensztejn, Z., Kuttler, F., Chuang, T.C., Moshir, S., Mougey, V., et al. (2005). *c-Myc induces chromosomal rearrangements through telomere and chromosome remodeling in the interphase nucleus.* Proc Natl Acad Sci U.S.A. 102, 9613-9618.

## List of Abbreviations

| | |
|---|---|
| 3D | Three-dimensional |
| AIDS | Acquired immune deficiency syndrome |
| ALT | Alternative lengthening of telomerase |
| APB | ALT-associated promyelocytic leukemia nuclear bodies |
| ATM | Ataxia telangiectasia mutated |
| BAX | BCL2-associated X protein |
| BBF cycle | Breakage-bridge-fusion cycle |
| BCL2 | B-cell CLL/lymphoma 2 |
| b-FGF | Basic fibroblast growth factor |
| BIR | Break-induced replication |
| CCD | Charge-coupled device |
| CDKN2A | Cyclin-dependent kinase inhibitor 2A |
| CLEM | Controlled light exposure microscopy |
| COX-2 | Cyclooxygenase-2 |
| CT | Chromosome territory |
| DNA | Deoxyribonucleic acid |
| EBV | Epstein Barr virus |
| EGFR | Epidermal growth factor receptor |
| FISH | fluorescence *in situ* hybridization |
| GAR1 | GAR1 ribonucleoprotein homolog (yeast) |
| H cells | Hodgkin cells |
| HER2/neu | Human epidermal growth factor receptor 2 |
| HPV | Human papilloma virus |
| H-Ras | Harvey sarcoma viral oncogene homolog |
| hTERC | Human telomerase RNA gene |

| | |
|---|---|
| hTERT | Human telomerase reverse transcriptase |
| IC | Interchromatin compartment |
| K-Ras | Kirsten sarcoma viral oncogene homolog |
| MALT | mucosa-associated lymphoid tissue |
| MMP | Metalloproteinase |
| NHP2 | NHP2 ribonucleoprotein homolog (yeast) |
| NOP10 | NOP10 ribonucleoprotein homolog (yeast) |
| PEV | Position effect variegation |
| PML | Promyelocytic leukemia |
| POT1 | Protection of telomeres protein 1 |
| PTEN | Phosphatase and tensin homologue |
| RAD52 | RAD52 homolog (S. cerevisiae) |
| RAP1 | Repressor activator protein 1 |
| RB | Retinoblastoma |
| RNA | Ribonucleic acid |
| RS cells | Reed-Sternberg cells |
| snRNP | Small nuclear ribonucleoprotein |
| TA | Telomeric aggregates |
| TGF-α | Transforming growth factor alpha |
| TIN2 | Second TRF1 interacting partner |
| TMM | Telomere maintenance mechanism |
| TP53 | Tumor protein 53 |
| TP73 | Tumor protein 73 |
| TRF1 | Telomere repeat-binding factor 1 |
| TRF2 | Telomere repeat-binding factor 2 |
| T-SCE | Telomere-sister chromatid exchange |
| VEGF | Vascular endothelial growth factor |

# Table of Contents

# I. INTRODUCTION

## 1.1 Historical Perspective of Nuclear Organization of Tumor Cells

David Paul Hansemann (1858-1920) made the first documentation of tumor initiation as the result of aberrant chromosome numbers in tumor cells. He observed asymmetric mitoses (Hansemann, 1890) and multipolar mitosis (Hansemann, 1891; Hansemann, 1893) in tumor cells . Theodor Boveri (1862-1915) extended Hansemann's views experimentally by using sea urchin eggs as his experimental model. He published this seminal work, "On Multipolar Mitosis as a Means to Analyze the Cell Nucleus" in 1902 (Boveri, 1902). He concluded that tumor formation was the result of multipolar mitosis which led to chromosome anomalies. He postulated that aberrant nuclear organization was linked to tumor initiation.

## 1.2 Tumorigenesis

Tumorigenesis is a multistep process that recapitulates Darwinian evolution, in which successive genetic alterations lead to transformation of normal cells into cancer cells (Foulds, 1957; Nowell, 1976). Hanahan and Weinberg defined six hallmarks of cancer: self-sufficiency in growth signals, insensitivity to anti-growth signals, evading apoptosis, limitless replicative potential, sustained angiogenesis, and tissue invasion and metastasis (Hanahan and Weinberg, 2000). Different genetic alterations that contribute to the characteristics of cancer have been identified in various tumor types. Genes

such as *EGFR* (Gibault et al., 2005; Hirsch et al., 2009; Rimawi et al., 2010; Ryott et al., 2009), *HER2/neu* (Choi et al., 2009; Hirsch et al., 2009; Skagias et al., 2009; Slamon et al., 1989), *cyclin D1*(Hadzisejdic et al., 2010; Lee et al., 2010; Liu et al., 2008) and *TGF-α* (Baek et al., 2009) can be over-expressed in tumor cells and thus impart self-sufficiency in growth signals. Tumors are insensitive to anti-growth signals from tumor suppressor genes such as *TP53* (Green and Kroemer, 2009; Riley et al., 2008; Yee and Vousden, 2005), *Rb* (Longworth and Dyson, 2010), *CDKN2A* (Bradley et al., 2006; Haller et al., 2008), and *PTEN* (Guney et al., 2007; Li et al., 2009). Genes involved in the regulation of apoptosis include *BAX* , *BCL2*, *Bcl-X* (Porichi et al., 2009; Zhang et al., 2009), and *Survivin* (Krepela et al., 2009; Lin et al.). Overexpression of genes such as *hTERT* give limitless replicative potential (Califano et al., 1996). Genes involved in angiogenesis include *b-FGF* (Marzioni et al., 2009), *COX-2* (McCormick et al., 2010), and *VEGF* (Zhang et al., 2010). The invasion-metastasis cascade is a series of steps involving primary tumor formation, local invasion, intravasation, extravasation, micrometastases and eventually macroscopic metastases (Fidler, 2003; Gupta and Massague, 2006; Thiery, 2002). Reduced expression of *beta-catenin* (Hsu et al., 2010) and *E-cadherin* (Hsu et al., 2010), or overexpression of *metalloproteinases (MMPs)* are associated with tumor invasion and metastasis (Del Casar et al., 2009; Germani et al., 2009; Szarvas et al., 2010).

Since Hanahan and Weinberg introduced the concept of the six hallmarks of cancer in 2000, additional hallmarks such as inflammation have been

proposed. The concept of a seventh hallmark, an inflammatory microenvironment, was first introduced in the 19th century by Rudolf Virchow (Balkwill and Mantovani, 2001) and, while its popularity waned for more than a century, it has become a generally accepted paradigm (Balkwill et al., 2005; Balkwill and Mantovani, 2001; Coussens and Werb, 2002; Karin et al., 2006; Mantovani et al., 2008). Recent studies have revealed that chronic inflammatory conditions have triggered cancer development. Examples of infections include human papilloma virus (HPV) for head and neck and cervical cancers (Gillison et al., 2000), Epstein Barr virus (EBV) for nasopharyngeal cancer (Gullo et al., 2008) and Hodgkin's lymphoma (Kapatai and Murray, 2007), *Helicobacter pylori* for gastric cancer (Machado et al., 2010) and mucosa-associated lymphoid tissue (MALT) lymphoma (Zullo et al., 2010), *Schistosomiasis* for bladder cancer (Casella et al., 2009), and hepatitis virus B and C for hepatocellular carcinoma (Neuveut et al., 2010). Autoimmune diseases involved in cancer development include Hashimoto's disease for thyroid cancer (Lee and Hasteh, 2009) and inflammatory bowel disease for colon cancer.

### 1.3 Genomic Instability

Genomic instability is defined as genetic alterations that affect the normal genetic and chromosomal organizations and functions. Genomic instability is broadly classified into structural and numerical genomic instability, and it ranges from single nucleotide mutations to gross chromosomal aneuploidy (Mai and Mushinski, 2003).

Structural genomic instability comprises point mutations, microsatellite instabilities, deletions, amplifications, duplications, translocations, and inversions of genes and chromosomes. On the other hand, numerical genomic instability, or aneuploidy, corresponds to an abnormal number of a chromosome in a cell, and extends from nullisomy to polysomy. When both structural and numerical genomic instabilities occur concurrently, it is termed karyotypic instability (Mai and Mushinski, 2003). In addition to karyotypic instability, more than one type of structural genomic instability is seen in various tumors throughout the progression of tumors.

Genomic instability is commonly seen in malignant transformation of cells, even though it is also found in normal and premalignant cells. Genomic instability can be induced by drugs, clastogens, deregulation of oncoproteins such as RAS and c-MYC, growth factors and genes responsible for cell cycle machinery, and double-stranded DNA breaks, which can induce gene amplification, deletions, and rearrangement, leading to loss of heterozygosity and translocations (Wright et al., 2009).

### 1.3.1 Cancer and Genomic Instability

The available evidence suggests that acquisition of the hallmarks of cancer during initiation and progression of cancer is through changes in the genomes of cancer cells, either directly or indirectly. In normal cells, the genome maintenance machineries such as apoptosis, cell cycle control and DNA repair machinery ensure that mutations are rare events that are unlikely to occur within

a human life span. However tumor genomes have acquired increased mutability during tumor progression (Loeb, 1991). Malfunctioning of the genome maintenance machinery can explain this increased mutability (Lengauer et al., 1998). These phenotypes, including microsatellite instability and chromosomal instability, are often seen in the karyotype of cancer cells, where there is an imbalance between the mechanisms of cell-cycle control and mutation rates within aberrant genes. Examples include ataxia telangiectasia, a disease that results from mutations in the ATM gene, a cell cycle checkpoint gene. Nijmegen breakage syndrome is also a disease characterized by chromosomal and genomic instability. Moreover, DNA damage repair genes are lost in different tumors. Their loss of function allows genomic instability and the generation of consequently mutant cells with selective advantages. Mutations of tumor suppressor genes such as *Rb* (Shay J Biochim Biopys Acta, 1072:1-7), *TP53* (Zilfou 2009) and *TP73* (Anselmo et al., 2009) can also increase genomic instability

### 1.4 c-*Myc*

*c-Myc* is a proto-oncogene involved in ≥ 70% of human cancer (Beckman and Loeb, 2005; Nesbit et al., 1999). It was first identified as the human homologue of avian retroviral oncogene in 1981. Since its discovery, it has been studied intensively in a wide spectrum of fields, including but not limited to molecular biology of cancer (Kuttler and Mai, 2006; Meyer and Penn, 2008). The overexpression of *c-Myc* in many human cancers is accomplished by a variety of molecular strategies. These include chromosomal translocations in Burkitt and

AIDS-related lymphoma, gene amplification in breast and prostate cancer, enhanced transcription of structurally normal *c-Myc* gene in colorectal cancer and increased transcriptional efficiency of *c-Myc* transcripts in multiple myeloma (Nesbit et al., 1999). Although point mutations in the *c-Myc* coding region are occasionally seen, particularly in Burkitt lymphoma, the vast majority of tumors express only the wild type protein, thus attesting to its primacy in mediating transformation (Bhatia et al., 1993; Lindstrom and Wiman, 2002; Nesbit et al., 1999).

### 1.4.1 *c-Myc* and Genomic Instability

*c-Myc* is a transcription factor and replication factor that alters the expression of hundreds of downstream target genes, many of them are either oncogenes or tumor suppressor genes (Guffei et al., 2007; Guijon et al., 2007; Kuschak et al., 2002; Prochownik, 2008). There are 2 types of transformation by *c-Myc* with overlapping pathways. The first type, “acute” transformation, is rapid, efficient, and requires no cooperating oncogenes (Stone et al., 1987) in *in vitro* transformation that only found in certain immortalized rodent cell line such as Rat1a fibroblasts (Stone et al., 1987). While transformation of primary rodent fibroblasts *in vitro* is rapid, over-expression of *c-Myc* alone is not sufficient and requires the contribution of another cooperating oncogene such as mutant *H-Ras* or *K-Ras* (Lee et al., 1985).

The second type, “chronic” transformation, is observed *in vivo*. The “chronic” form of *in vivo* transformation by c-*Myc* is a rare event that requires the

acquisition of multiple mutations in other genes affecting cell cycle, senescence, and apoptosis. By greatly accelerating the intrinsic mutation rate at several levels, c-*Myc* increases the likelihood that these additional mutational "hits" will occur. c-*Myc* deregulation is insufficient and other non-*Ras* oncogenes and/or the inactivation of tumor suppressors are required.

In addition to its direct action on chronic transformation, c-*Myc* also plays an indirect role in inflicting DNA damage through "mutator phenotype" (Beckman and Loeb, 2005), which accelerates the rate of acquisition of these additional genetic hits. Among the types of genomic instability mediated by c-*Myc* are: 1) single nucleotide substitutions and double-stranded breaks arising via the induction of reactive oxygen species, 2) gene amplification and generation of extrachromosomal elements, 3) numerical chromosomal defects resulting from aberrant DNA synthesis and defects in the mitotic spindle checkpoint, 4) initiation of illegitimate replication of the ribonucleotide reductase *R2* gene (Kuschak et al., 2002) and 5) regulation of differentiation and maintenance of neural stem cell as well as tumorigenic potential of glioblastoma when both *p53* and *PTEN* are deleted (Zheng et al., 2008). These non-mutually exclusive activities ensure a constant and varied source of genotoxic insults and suggest that c-*Myc* overexpression imposes a "mutator phenotype". This may be an early and necessary requirement for the initial steps in chronic transformation as well as for subsequent evolutionary changes that produce important tumor behaviors such as invasiveness, metastasis, and acquisition of chemotherapy resistance.

## 1.5 Telomeres

Telomeres are specialized chromatin structures located at the end of the linear chromosome containing repetitive DNA sequences (5’ – TTAGGG- 3’) and a nucleoprotein complex. This complex is termed the telosome and protects the chromosomes from rearrangements and triggering DNA repair pathways. There are 6 proteins associated with the telomeres which are collectively termed the shelterin (de Lange, 2005). It consists of TRF1, TRF2, and POT1 that will directly recognize the TTAGGG repetitive sequence. They are interconnected to the other three proteins TIN2, TPP1 and RAP1.

### 1.5.1 The End Replication Problem

Semiconservative replication of DNA presents a unique problem: the process only works in the 5' to 3' direction, and DNA polymerase requires binding of an RNA primer. Olovnikov and Watson predicted the consequences of this long before the telomere was characterized and termed it the end-replication problem. It anticipated the loss of a small 5' nucleotide segment as DNA synthesis took place, with progressive replication-induced telomere shortening (Olovnikov, 1973; Watson, 1972).

The 3' end of the DNA molecule is replicated continuously to the very end, having started at the opposite 5' terminus. However, synthesis of the lagging strand (also in the 5' to 3' direction) is discontinuous because of the requirement for RNA primer binding and unidirectional growth of the new strand. Upon

removal of the RNA primers, the gaps in the discontinuous lagging strand are filled in and ligated. However, there is no provision for such a process at the immediate 5' end, thus leaving a gap. Since the DNA duplex is antiparallel, each daughter molecule will be shortened on its 5' end after replication, with successively shorter daughter chromosomes resulting from additional cycles of cell division.

The end-replication problem, along with other endogenous or exogenous factors, causes shortening of telomeres by ~50-200 base pairs in each cell division (Lansdorp, 2000). Telomere erosion limits the replication capacity of somatic cells that do not express telomerase (Harley et al., 1990; Lindsey et al., 1991). Once the telomeres are shortened to a critical length, cells enter a state of replicative arrest called senescence (Harley et al., 1992; Hayflick, 1965). Senescence is an aging process that protects cells from genomic instability and transformation as a result of telomere dysfunction. Stem cells and germ cells express telomerase and therefore are able to maintain their telomere length and escape senescence. Senescence can be bypassed during tumor development (Campisi, 2000).

Various lines of evidence have shown that several diseases including cancer can be driven by shortening of telomeres in the absence of telomerase. When telomere end protection is compromised, DNA damage response occurs at the chromosome end. This explains replicative senescence. Telomeres can also become dysfunctional through another mechanism, alterations in telomere-

binding proteins, the shelterins. And finally, conditional c-*Myc* deregulation leading to the formation of telomeric aggregates (Louis et al., 2005) was described previously and is part of my thesis.

### 1.5.2 Telomerase and Alternative Lengthening Pathway (ALT)

One of the hallmarks of cancer is limitless replicative potential, which could be accomplished through activation of telomerase (Hanahan and Weinberg, 2000). Cancer cells can maintain telomere length through one of two telomere maintenance mechanisms (TMM): active telomerase or alternative lengthening of telomerase (ALT). Kim et al. surveyed several tumor types and have shown that ~85% of tumors express telomerase and maintained a stable and homogenous telomere length and therefore avoid replicative senescence (Kim et al., 1994). The remaining ~15% of tumors either do not maintain telomere length or activate the ALT mechanism (Bryan et al., 1995). Utilization of different TMM is tumor type-specific. Kammori et al. had demonstrated that ~100% of colon adenocarcinomas express telomerase (Kammori et al., 2002). In contrast, a high proportion of sarcomas utilized ALT mechanism, such as 47% in osteosarcomas, 25% in liposarcomas, and 34% in astrocytomas (Costa et al., 2006; Henson et al., 2005; Johnson et al., 2005). There is evidence that both TMMs can be activated in the same cell line and a small number of tumors (Costa et al., 2006; Johnson et al., 2005). Similarly, ALT positive (ALT +) primary tumors can give rise to telomerase positive (telomerase +) secondary tumors and vice versa.

Human telomerase is a ribonucleoprotein complex that is required for overcoming the end-replication problem. It adds the six nucleotide repeats (TTAGGG) to the chromosome ends by utilizing the reverse transcriptase (hTERT) and the RNA template (hTERC), as well as the associated proteins including dyskerin, NOP10, NHP2, and GAR1.

The recombination-based ALT mechanism was first described in *Saccharomyces cerevisiae* that lack one of the essential components of telomerase (TLC1 or EST1) (Le et al., 1999; Lundblad and Blackburn, 1993; McEachern and Blackburn, 1995). A majority of telomerase negative yeast died after entering crisis. Only few clones with RAD52, which is required for double strand break repair and homologous recombination (Lundblad and Blackburn, 1993), were selected.

A telomere tagging experiment performed by Dunham et al. (Dunham et al., 2000) was the first evidence demonstrating that the mechanism underlying ALT in human cells is based on a recombination-like process. The phenotype of human ALT+ cell lines was first described by Murnane et al. and Bryan et al. (Bryan et al., 1995; Murnane et al., 1994). A proportion of ALT+ cells contain large specialized ALT-associated promyelocytic leukemia nuclear bodies (APBs) (Yeager et al., 1999). These APBs contain telomeric DNA, telomere repeat binding factors 1 and 2 (TRF1 and TRF2) and associated proteins, which can be distinguished from other promyelocytic leukemia (PML) bodies in the same cell and in other cell types.

ALT+ cell lines and tumors show heterogeneous telomere length, extrachromosomal circular and linear telomeric DNA (Tokutake et al., 1998), APBs (Yeager et al., 1999), a high frequency of post-replication exchanges in telomeres, also known as telomere-sister chromatid exchange (T-SCE) (Laud et al., 2005), and high instability at a GC-rich minisatellite, MS32 (D1S8) (Jeyapalan et al., 2005). There is a link between the minisatellite instability and the mechanism that underpins ALT. Single molecule analysis of telomeric DNA from ALT+ cell lines and tumors has revealed complex telomere mutations that have not been seen in cell lines or tumors that express telomerase. These complex telomere mutations cannot be explained by T-SCE but must arise by another inter-molecular process. The break-induced replication (BIR) model may explain the observed high frequency of T-SCE and the presence of complex telomere mutations (Dunham et al., 2000).

### 1.5.3 Telomere and Genomic Instability

Defects in DNA repair and the DNA damage response pathway, as well as structural and functional disruption of telomeres are among the leading causes of genomic instability in cancer and aging (Stewenius et al., 2005). Telomeres are crucial for the preservation of chromosome integrity and controlled cell proliferation (Blackburn, 2001; de Lange, 2002). Telomere-driven instability can promote both structural and numerical chromosomal aberrations (Pampalona et al.). A minimal length of telomeric DNA repeats and proper recruitment of telomere binding proteins are necessary to preserve telomere function (de

Lange, 2005; Liu et al., 2004). In addition, the acquisition of a heterochromatic structure at telomeres is essential for the maintenance of telomere length homeostasis (Blasco, 2007). Over-expression of c-*Myc* leads to telomeric dysfunction and the subsequent formation of telomeric aggregates and dicentric chromosomes, eventually inducing breakage-bridge-fusion (BBF) cycles (Louis et al., 2005).

## 1.6 Three-Dimensional Organization of Chromosomes

The mammalian nucleus has a non-random organization of the genome, nuclear compartments, and nuclear proteins (Misteli, 2007; Schneider and Grosschedl, 2007). Studies have shown that the mammalian nucleus is temporally, spatially, and functionally organized and containing numerous nuclear bodies and non-randomly positioned genome domains (Dundr and Misteli, 2001; Kress et al., 2010). The 3D arrangement of the distinct chromosome territories is linked to genomic function and the global regulation of gene expression (Berezney, 2002; Kumaran et al., 2008; Lanctot et al., 2007; Marella et al., 2009; Misteli, 2005; Misteli, 2007; Stein et al., 2003a; Stein et al., 2003b). However, its physiologic function has not been well understood until recently when Solovei et al. demonstrated for the first time that non-random nuclear order plays an important role in physiologic function of retina of nocturnal animal (Solovei et al., 2009).

### 1.6.1 Nuclear Compartments and Functional Relevance

The genomic function can be spatially organized into three hierarchical levels in a cell: the organization of the chromatin fiber into higher order, the spatial and temporal organization of nuclear processes, and the spatial arrangement of genomes within the nuclear space (Misteli, 2001; Misteli, 2007). The double-stranded DNA helix is folded into higher-ordered structures that eventually form the three-dimensional conformation of chromosomes (Misteli, 2007; Woodcock, 2006). In addition to DNA arrangement, the cellular factors such as replication and transcription machineries are also spatially compartmentalized and distributed in specific nuclear domains (Misteli, 2001).

Most nuclear events occur in the specific, spatially defined compartments that are generally proteinaceous nuclear bodies or chromatin domains (Lamond and Spector, 2003; Misteli, 2005). The most prominent nuclear bodies include: the nucleolus, which is the site of transcription and processing of ribosomal RNA; the splicing factor compartments, which act as storage assembly sites for spliceosomal components; the Cajal body, which is the proposed site of small nuclear ribonucleoprotein (snRNP); and the promyelocytic leukemia (PML) body, which is of unknown function. These nuclear bodies are self-organized into well-defined yet dynamic compartments (Misteli, 2005). Different types of cells and tissues have different preferential positions of nuclear bodies within the nucleus. Similarly, the positions of the nuclear bodies change in different physiological and pathologic processes.

Genomes are non-randomly arranged in the 3D space of the nucleus. Several studies have suggested that the nucleus is compartmentalized and alteration of the 3D nuclear organization affects genomic function (Dechat et al., 2008; Goldman et al., 2002; Gonzalez-Suarez et al., 2009; Gruenbaum et al., 2005; Misteli, 2007). Thomas Cremer described that chromosomes occupy discrete territories in the cell nucleus and contain distinct chromosome-arm and chromosome-band domain (Cremer and Cremer, 2001). Interphase chromosomes are organized into chromosome territories (CTs) in the nucleus (Cremer and Cremer, 2001; Cremer et al., 2006; Spector, 2003). Each individual CT has a non-random location and orientation within the interphase nucleus and no overlapping between CTs. Each CT occupies a spatially defined subvolume in the nuclear space. Using fluorescence *in situ* hybridization, the CTs are visualized *in situ* (Lichter et al., 1988). CTs with different gene densities occupy distinct nuclear positions. Euchromatins are less-condensed and gene-rich. On the other hand, heterochromatins are open chromatin regions with gene-poor regions. Gene-rich chromosomes are positioned preferentially towards the center of the nucleus while the gene-poor chromosomes are located toward the periphery. In addition, the arrangement of chromosomes within the nucleus appears to be tissue-specific (Cremer et al., 2003; Meaburn and Misteli, 2007; Parada et al., 2004). Gene-poor, mid-to-late-replicating chromatin regions on chromosomes are enriched in nuclear compartments that are located at the nuclear periphery and at the perinucleolar region. A compartment for gene-dense, early-replicating chromatin is separated from the compartments for mid-

to-late-replicating chromatin. Chromatin domains with a DNA content of ~1 Mb can be detected in nuclei during interphase and in non-cycling cells. The interchromatin compartment (IC) contains various types of non-chromatin domains with factors for transcription, splicing, DNA replication and repair. The CT-IC model predicts that a specific topological relationship between the IC and chromatin domains is essential for gene regulation. The transcriptional status of genes correlates with gene positioning in CTs. A dynamic repositioning of genes with respect to centromeric heterochromatin has a role in gene silencing and activation. Various computer models of CTs and nuclear architecture make different predictions that can be validated by experimental tests. Comprehensive understanding of gene regulation requires much more detailed knowledge of gene expression in the context of nuclear architecture and organization (Cremer and Cremer, 2001).

#### 1.6.1.1 3D Nuclear Organization and its Cellular Functions

It has been proposed that clustering of genes in transcription hot spots plays a role in their regulation and expression (Fraser and Bickmore, 2007; Lanctot et al., 2007), the association of translocation and the relative positioning of chromosomes (Misteli, 2007), replication timing and gene positioning (Gilbert, 2001), and X-inactivation through physical interactions between X chromosomes (Erwin and Lee, 2008).

Gene positioning is found in non-random patterns. Positioning-induced silencing is the phenomenon of position effect variegation (PEV). A gene is

silenced when inserted into heterochromatin genome region. In human cells, the translocation partners for several lymphoma have been found in closer spatial proximity (Roix et al., 2003). These observations suggest that non-random spatial positioning of genome can contribute to what genome regions interact with what other regions (Parada et al., 2002).

#### 1.6.1.2 3D Nuclear Organization and its Physiologic Functions

Solovei et al. has shown that the physiologic functions of rod cells are closely related to the 3D organization of the interphase nucleus (Solovei et al., 2009). The nuclear architecture of rod photoreceptor cells is different in nocturnal and diurnal mammals. In diurnal retinas, the rods possess the canonical architecture with euchromatin located in the nuclear center while the heterochromatin is situated at the nuclear periphery. On the other hand, the rods of nocturnal retinas have an inverted pattern, where heterochromatin resides toward the nuclear interior while euchromatin, nascent transcripts, and splicing machinery line the nuclear border. The differences of the two patterns suggest that the canonical architecture in eukaryotic nuclei result in more flexible chromosome arrangements, facilitating positional regulation of nuclear functions.

### 1.6.2 Telomere Compartmentalization

Telomere compartmentalization for telomere function has been studied in yeast (Akhtar and Gasser, 2007). However, the underlying mechanism for the spatial organization of telomeres in the mammalian nucleus still remains elusive.

In addition, the relationship between the arrangement of mammalian telomeres and telomere biology is not well understood. Gonzalez-Suarez et al. showed that loss of A-type lamins changes the nuclear distribution of telomeres away from the nuclear centre and towards the periphery. The latter results in telomere shortening, defects in telomeric heterochromatin, and increased genomic instability (Gonzalez-Suarez et al., 2009).

## 1.7 Molecular Imaging

Light microscopy has been used for centuries to visualize structures too small to see with the naked eyes. Optical microscopy is an important tool in the investigation of cellular process and structures. It allows one to work with intact samples including living cells and to see samples with the naked eye.

### 1.7.1 Light Microscopy

Robert Hooke (1638-1703) published the Micrographia in 1665, which is the first book on microscopy (Hooke, 1665). He refined compound microscopy, which consisted of a stage, a light source and three optical lenses. Among numerous detailed observations made with his microscope, he termed the pores of the cork as “cells”. The introduction of multiple lenses increased issues with spherical and chromatic aberration. A simple microscope containing a single convex lens was first developed by Van Leeuwenhoek (1632-1723) (van Leeuwenhoek, 1800). He was the first to observe sperm cells and bacteria and

protozoa in water. Using a simple microscope was superior for observation until the advent of achromatic lens became widely available in nineteenth century.

### 1.7.2 Resolution of Light Microscopy

Diffraction occurs as the light enters the lens aperture. A diffraction pattern in the image which has central white spot with surrounding white rings separated by dark rings is known as the Airy disc, as described by George Airy in 1835 (Airy, 1835). The diffraction barrier dictates the limit of resolution of light microscopy.

Resolution is the ability to discern 2 points distinctively, and it is described by Abbe in 1873 (Abbe, 1873). The Abbe's formula published in 1873 stated:

$$D=\lambda/2\ n \sin a \text{ where}$$

D= minimum distance between 2 objects that reveals them as separate entities

λ= wavelength of the light

n sin a = numerical aperture of the lens.

The limit of optical resolution of a conventional light microscope is approximately ½ of wave-length. This is approximately 200 nm.

### 1.7.3 Fluorescent Dyes and Fluorescent Microscope

Fluorescence was first defined by Stokes who described it as light emission induced during excitation (Stokes, 1852). Fluorescence provides

infinite contrast with the right equipment. The fluorescent microscope was first constructed by Oskar Heimstädt in 1911 (Heimstädt, 1911). Initial limitations of fluorescence microscopy included reliance on auto-fluorescence of the images object and the need for transmitted illumination and darkfield condenser. The first hurdle was addressed via development of fluorochrome or secondary fluorescence (Freund, 1969). This involves attaching exogenous fluorescence chemicals to the samples. Epi-fluorescence microscope was developed in 1929 (Ellinger and Hirt, 1929). The light source lies on the same side of the sample as the objective, and excitation and emission light pass through the objective. This allows more efficient sample excitation and imaging of opaque objects. Another advance occurred in 1967 with development of dichromatic mirrors or beam splitters (Ploem, 1967). Dichromatic filters reflect a narrow width of wavelengths while transmitting all others, allowing illumination of the sample with precise wavelength. The reflected shorter wavelength excitation light enters the objective which also functions as a condenser to allow even excitation of the sample. The emitted longer wavelength fluorescent light is collected by the objective and passed through the dichromatic mirror and a barrier filter to the eyepiece.

### 1.7.4 The Charge-Coupled Device (CCD)

The charge-coupled device (CCD) was invented and published in 1970 by Boyle and Smith (Boyle and Smith, 1970). The CCDs are solid-state image sensors that make use of the photoelectric effect. This allows transformation of

light or photons into electric signals so that light can be captured and stored electronically. This technology is used in many fields including digital photography for research or recreation, and endoscopy for medicine or industrial purposes. Use of CCD in digital imaging of fluorescence was first described in 1986 (Connor, 1986). The study was to image free calcium levels in individual central nervous system cells from rat embryo. From digital images captured, the author was able to show high levels of calcium at the growing tips of the central nervous system cells.

### 1.7.5 Deconvolution Algorithm

The conventional fluorescence microscope contains light from throughout the specimen. The out-of-focus fluorescence confounds what is present in the focal plane. A means to achieve clarity and to minimize artifact of images is by applying a mathematical processing method known as deconvolution algorithm to the stack of images. The deconvolution algorithm determines how much out-of-focus light is expected given the optics in use and then seeks to reassign the diffracted light to its points of origin in the specimen. With the use of deconvolution, reconstruction of a three-dimensional object is possible by taking a sequential stack of images captured on films or digital image sensors. The deconvolution algorithm was first used in 1983 and allowed for the recovery of detail of the polytene nucleus of the *Drosophila melanogaster* salivary gland from fluorescent images captured on films (Agard and Sedat, 1983).

Different deconvolution algorithms have been developed. The constrained iterative deconvolution algorithm was chosen for the 3D work performed in this thesis (Schaefer et al., 2001) to restore 3D images.

### 1.7.6 3D Microscopy

With the convergence of different disciplines of science including the development of the CCD digital camera, deconvolution algorithm, and automated FISH microscope, the ability to visualize microscopic objects in 3D space is greatly enhanced. Through collaboration with physicists from the Netherlands, the Teloview program has been developed to perform quantitative analysis of three-dimensional images of telomeres and chromosomes (Vermolen et al., 2005).

The importance of telomeres and the development of CCD technology is highlighted by the Nobel prize committee members who awarded the pioneers in the fields of telomeres and CCD the Nobel prizes in 2009. Elizabeth Blackburn, Jack Szostak, and Carol Greider were awarded the Nobel Prize in Physiology or Medicine for their discovery of the structure and function of telomeres. Willard S. Boyle and George E. Smith were awarded the Nobel Prize in Physics for the invention of the CCD sensor.

# II. Published Manuscripts

## 2.1 The three-dimensional organization of telomeres in the nucleus of mammalian cells.

Access the publication online is available via the following link:

http://www.biomedcentral.com/1741-7007/2/12

### Rationale of the Investigation

Genomic instability is a characteristic of the tumor cell. It includes numerical and structural alterations of chromosomes. Numerical changes such as amplifications, deletions, and duplications have been widely studied. However, aberrations of temporal and spatial organization of chromosomes in three-dimensional (3D) space and dysregulation of transcription, replication, and stability of the genome in tumor cells have yet to be investigated further.

### Objectives

To establish the telomere organization in 3D space of interphase nuclei.

To evaluate for differences in telomeric organization in normal and tumor cells.

### Hypothesis

Telomeres are arranged in a non-random and dynamic fashion in the 3D space of a normal cell. In tumor cells, telomere organization is disrupted as a result of genomic instability.

## Summary of Findings

*Nonrandom dynamic 3D telomere organization in a normal nucleus*

The 3D telomere organizations of normal, immortalized and tumor cells have been examined in different cell lines and various human primary tissues. Telomeres are organized in non-random and non-overlapping arrangement in the 3D space of a normal nucleus.

*3D telomere organization is disrupted in the nucleus of a tumor cell*

Telomeres are distributed non-randomly in the 3D space of a mammalian nucleus throughout the cell cycle. However, this organization is disrupted in tumor cells with the formation of telomeric aggregates of various numbers and sizes.

## My Contributions to the Work

I was one of the first ones to make the initial observation of non-random telomere organization in normal and immortalized cell in 3D space. I had also made additional observation that telomeric aggregations were a common denominator in various tumor cell lines and tissues.

To study the 3D telomere organization throughout the cell cycle of a normal mammalian nucleus, I planned the experiments and performed 3D telomere fluorescence *in situ* hybridization (FISH) followed by the quantitative analysis of telomere distribution using the TeloView programme developed by

our collaborators in the Netherland. I discovered that telomeres were arranged in a cell-cycle dependent fashion, with the formation of the telomeric disk in the late G2 phase.

I obtained all head and neck cancer tissues from patients. Prior to the surgery, I described the study to the patients, answering their questions, and obtained the consents prior to the surgery. I also processed the tissues for the study by preparing the fresh frozen sections for FISH analysis. I also prepared clinical data and correlated the experimental result with the clinicopatholgoic parameters.

BMC Biology

BioMed Central

Research article

Open Access

# The three-dimensional organization of telomeres in the nucleus of mammalian cells

Tony Chih Yuan Chuang[†1,3], Sharareh Moshir[†1,2], Yuval Garini[*†4], Alice Ya-Chun Chuang[1], Ian T Young[4], Bart Vermolen[4], Richard van den Doel[4], Virginie Mougey[5], Mathilde Perrin[5], Martina Braun[1], Paul Donald Kerr[3], Thierry Fest[5,6], Petra Boukamp[2] and Sabine Mai[1]

Address: [1]Manitoba Institute of Cell Biology, CancerCare Manitoba, University of Manitoba, 675 McDermot Avenue, Winnipeg, MB, R3E 0V9, Canada, [2]German Cancer Research Centre, Division of Genetics of Skin Carcinogenesis, Im Neuenheimer Feld 280, 69120 Heidelberg, Germany, [3]Department of Otolaryngology Head and Neck Surgery, Health Sciences Centre, GB421-820 Sherbrook Street, Winnipeg MB, R3A 1R9, Canada, [4]Delft University of Technology, Faculty of Applied Sciences, Department of Imaging Science & Technology, 2628 CJ Delft, The Netherlands, [5]Hematology Department, IETG Laboratory, University Hospital Jean Minjoz, 25030 Besançon, France and [6]Present address: Hematology Laboratory, University Hospital Pontchaillou, 35033 Rennes, France

Email: Tony Chih Yuan Chuang - tcychuang@hotmail.com; Sharareh Moshir - s.moshir@dkfz.de; Yuval Garini* - Y.Garini@tnw.tudelft.nl; Alice Ya-Chun Chuang - alicechuang@hotmail.com; Ian T Young - young@ph.tn.tudelft.nl; Bart Vermolen - vermolen@ph.tn.tudelft.nl; Richard van den Doel - richard@ph.tn.tudelft.nl; Virginie Mougey - virginie.mougey@voila.fr; Mathilde Perrin - mathilde-perrin@caramail.com; Martina Braun - tina-braun@gmx.net; Paul Donald Kerr - pkerr@exchange.hsc.mb.ca; Thierry Fest - thierry.fest@univ-rennes1.fr; Petra Boukamp - P.Boukamp@dkfz-heidelberg.de; Sabine Mai - smai@cc.umanitoba.ca

* Corresponding author †Equal contributors

Published: 03 June 2004

BMC Biology 2004, 2:12

Received: 10 March 2004
Accepted: 03 June 2004

This article is available from: http://www.biomedcentral.com/1741-7007/2/12



## Abstract

**Background:** The observation of multiple genetic markers *in situ* by optical microscopy and their relevance to the study of three-dimensional (3D) chromosomal organization in the nucleus have been greatly developed in the last decade. These methods are important in cancer research because cancer is characterized by multiple alterations that affect the modulation of gene expression and the stability of the genome. It is, therefore, essential to analyze the 3D genome organization of the interphase nucleus in both normal and cancer cells.

**Results:** We describe a novel approach to study the distribution of all telomeres inside the nucleus of mammalian cells throughout the cell cycle. It is based on 3D telomere fluorescence *in situ* hybridization followed by quantitative analysis that determines the telomeres' distribution in the nucleus throughout the cell cycle. This method enables us to determine, for the first time, that telomere organization is cell-cycle dependent, with assembly of telomeres into a telomeric disk in the G2 phase. In tumor cells, the 3D telomere organization is distorted and aggregates are formed.

**Conclusions:** The results emphasize a non-random and dynamic 3D nuclear telomeric organization and its importance to genomic stability. Based on our findings, it appears possible to examine telomeric aggregates suggestive of genomic instability in individual interphase nuclei and tissues without the need to examine metaphases. Such new avenues of monitoring genomic instability could potentially impact on cancer biology, genetics, diagnostic innovations and surveillance of treatment response in medicine.

## Background

Cancer is characterized by multiple alterations that affect the modulation of gene expression and the stability of the genome. These interconnected changes occur within the nuclei of cells that alter their three dimensional (3D) organization during tumor initiation and progression [1,2]. It seems reasonable to assume that the highly organized mammalian interphase nucleus is the structure that ascertains genomic stability. In line with these concepts, oncogenic activation remodels this nuclear order and sets the stage for genomic instability as we have recently measured for conditional c-Myc deregulation. The deregulated expression of c-Myc alters the 3D nuclear space of chromosomes and telomeres, and makes genomic rearrangements topologically feasible (Chuang *et al.*, in preparation).

Defining the structural organization of the interphase nucleus is, therefore, essential to our understanding of the 3D genome organization in the interphase nucleus. Such a study can be performed by fluorescence *in situ* hybridization (FISH). Two of the most attractive features of FISH measurements of the 3D nucleus organization are the ability to simultaneously visualize multiple targets and the structural organization of nucleus and cells, something that cannot be achieved by array-based methods.

The organization of the interphase nucleus has been studied since the late nineteenth century [3]. It is now well accepted that the position of chromosomes in the nucleus plays an important role in gene regulation [4]. Nevertheless, some controversy exists. Most laboratories have observed a non-random organization of chromosome territories [2,5,6] that has been conserved during evolution [7]. This has been further supported by studies that demonstrate an architectural stability of the chromosomal positions in the nucleus [8,9]. There are, however, different observations on chromosomal positions [10-15] as well as on positional changes of chromosomes during the cell cycle [16,17].

Recently, interest has also focused on telomeres, whose importance to genomic stability was recognized as early as the 1930s [18]. Capping the chromosomes, telomeres are responsible for chromosomal integrity [19] to prevent genomic instability [20]. Some reports have been published on the 3D organization of telomeres in the nucleus, mainly with regard to the distances of telomeres from the nuclear shell. Telomeres have been previously found at the nuclear edge [21], at the nuclear periphery [22], throughout the entire nucleus [13,23], in non-Rabl association [11], in association with the nucleolus [24] or in the nuclear matrix [25].

Telomere dynamics also have been studied in living human U2OS osteosarcoma cells [26]. Individual telomeres showed significant directional movements and telomeres were shown to associate with promyelocytic leukemia bodies in a dynamic manner. This means that telomere structure is dynamic, and may be important for both transcriptional processes and for stabilizing chromosome positions in the nucleus.

We have developed a method of studying the organization of the genome by analysis of the 3D organization of telomeres in the nucleus and their positional changes along the cell cycle, using flow-sorted living cells. This method enables us to determine, for the first time, that telomere organization is cell-cycle dependent, with assembly of telomeres into a telomeric disk in the G2 phase. Moreover, we show for tumor cells that the 3D telomere organization is distorted and that telomeric aggregates are formed. These results emphasize a non-random and dynamic 3D nuclear telomeric organization and its importance to genomic stability.

## Results and discussion

To study the organization and structure of the genome in the nucleus, we took the approach of labelling only the telomeres and measuring their 3D organization as indicators for chromosomal distribution. After the 3D fluorescent measurements, the data were analyzed with a programme that was developed for this study. The programme finds all the telomeres in the nucleus; their size, intensity and shape; and determines the telomeric organization inside the volume of the nucleus. One crucial property that we analyzed was the distribution of the telomeres inside the nuclear volume. We first segmented the nucleus and found the centre of each telomere. We then found the smallest convex set of polygons that contains all the telomeres (Fig. 1). This was done by using the Quickhull algorithm [27]. In most cases, we found that the volume contained by the telomeres resembles either a sphere or a flattened sphere (disk). It can be described as an ellipsoid with two similar radii ($a$=$b$) and a different third one ($c$; Fig. 2). Such a shape is called a spheroid. The level of flatness of the volume occupied by the telomeres can, therefore, be described by the ratio of the two radii that are different, $a$ (or $b$) and $c - a/c$. The larger the ratio, the more oblate (or disk-like) is the shape of the volume occupied by the telomeres, while $a/c \approx 1$ means that the volume is spherical.

The optical resolution and signal-to-noise ratio are presented in Fig. 3. The images of two neighbouring telomeres that are 1200 nm and 400 nm apart, and the corresponding intensity along the line connecting the pair, indicates the smallest telomere distance that can still

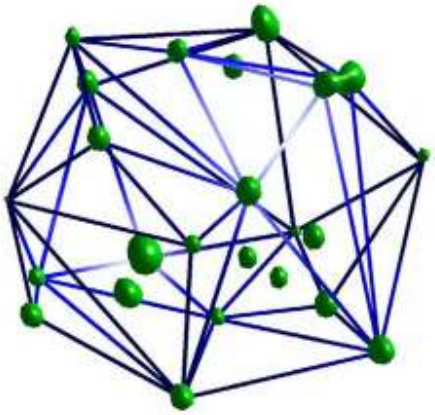

**Figure 1**
The distribution of the telomeres in the nucleus volume is found by fitting a convex set of polygons that contains all the telomeres. This volume usually looks like either a sphere or a disk and can be described as an ellipsoid.

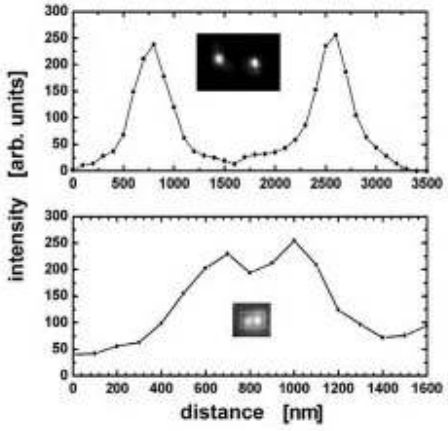


**Figure 3**
Demonstration of the signal-to-noise and spatial resolution of our measurements. The fluorescence intensity is bright (typical signal-to-noise ratio of 10:1). Two pairs of telomeres are shown, 1200 nm apart (top), which can be easily separated, and 400 nm apart (bottom). The inserts show the actual images.

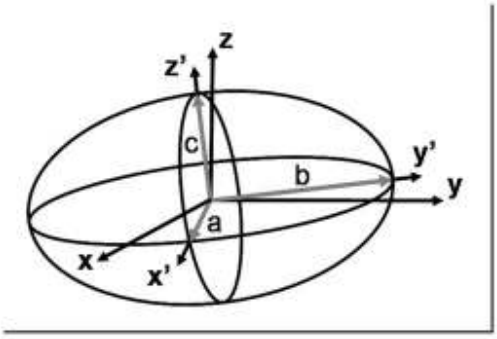


**Figure 2**
In general, the ellipsoid's main axes along *x'y'z'* do not coincide with the microscope-slide plane and optical axes *xyz*. Our programme finds an ellipsoid that contains all the telomeres and the size of its main axes *a,b,c*. In most of the cases the *x'y'* axes of the ellipsoid are similar, i.e. $a \approx b$. Therefore, the ratio *a/c* is a good measure of the flatness level of the ellipsoid and of the telomere organization inside the nucleus.

be unambiguously distinguished (approximately 200 nm).

It is expected that 80 telomeres will be observed in the interphase nucleus for normal mouse cells (92 for a normal somatic human cell), however, in our measurements we were usually able to identify approximately 40 separated telomere regions in each mouse cell (50 in human cells). Similar results have been described before [23,28]. This is probably due to neighbouring telomeres that are closer than the optical resolution (see Fig. 3), but it does not affect the analysis of the telomere distribution in the nucleus as long as the hybridization efficiency is high. This was verified by two-dimensional measurements of all the telomeres in a metaphase spread (using the same probe), where at least 90% of the telomeres are unambiguously observed (Fig. 4).

We first described the major observation of primary BALB/c mouse B lymphocytes that were studied along the cell cycle. These studies were followed by the analysis of immortalized cells. The lymphocytes were sorted according to their DNA content for the determination of the G0/G1, S or G2/M phases (see *Methods*).

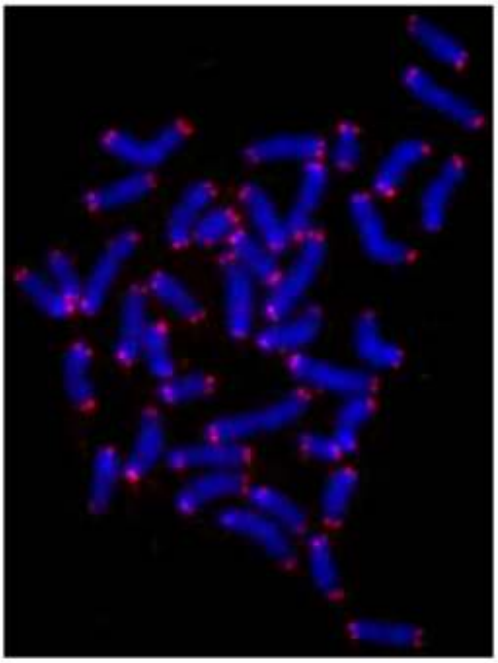

**Figure 4**
Metaphase plate prepared from fetal liver cells directly isolated from day 10 old mouse embryos. Metaphase chromosomes and spreads were prepared as described [30] and hybridized with a PNA-telomeric probe that was Cy3 labelled. More than 90% of the telomeres are clearly observed.

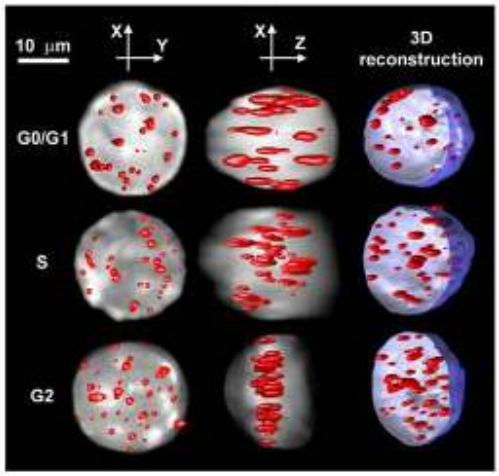


**Figure 5**
The distribution of telomeres in the nucleus of three typical cells selected from the G0/G1 phase (upper row), S phase (middle row) and G2/M phase (lower row). Each telomere distribution is shown from a top view (the *XY* plane), along the optical axis *Z* (left column), from a side view (*XZ* plane) as observed along the *Y* axis (centre column) and as a 3D image of the telomeres in an open nucleus (right column). When shown from the top and side views, the telomeres are displayed on top of the projected image of the nucleus. This projection demonstrates the extent of the chromatin (and therefore chromosomes) and defines the volume and borderline of the nucleus.

By analyzing cell-cycle sorted primary mouse lymphocytes we found that the 3D telomere organization changes during the cell cycle. Telomeres are widely distributed throughout the nucleus in the G0/G1 and S phases with a calculated *a/c* ratio of 0.9 ± 0.4, which means a spherical-like volume of distribution. However, during G2, telomeres are not observed throughout the whole nucleus. Their 3D organization changes, with all the telomeres assuming a central structure that we call the telomeric disk, which has never been reported before. In this ordered structure, all the telomeres align in the centre of the nucleus as cells progress into the late G2 phase. The *a/c* ratio they assume is 6.0 ± 2.0, which means a very flat disk (almost a coin shape).

Typical lymphocytes from different phases are shown in Fig. 5. The *a/c* ratio of these cells in the G0/G1, S and G2/M phases is 0.8, 0.8 and 6, respectively, and clearly shows the correlation of the *a/c* ratio with the telomere distribution and the organization of the telomeric disk that we found in the G2 phase. The elongation of the telomeres along the *Z* axis (the optical axis) relative to the *XY* plane has the same ratio as the point spread function of our system and results from the poorer optical resolution along the optical axis. However, this has a very small effect on the shape of the whole nucleus.

Similar results have been observed in primary human lymphocytes, primary human fibroblasts and in normal human epithelial tissue (see additional file for more data). This suggests that chromosomes assume a very precise order that pre-aligns them prior to the onset of mitosis. In order to ascertain that the telomeric disk was not the result of a distorted nucleus, our analysis programme

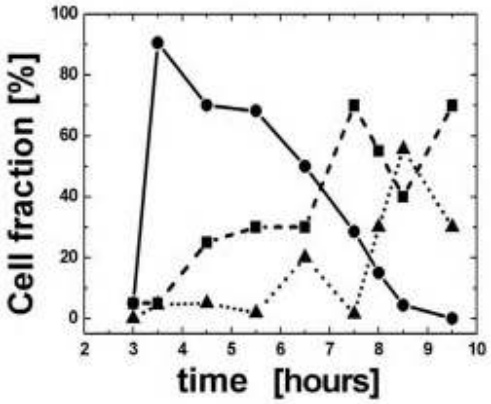


**Figure 6**
BrdU-positive cells were live sorted and synchronized in the S phase. They were harvested from a culture at time intervals of 3.5–9 hours. The cells were then fixed for 3D analysis. For each time point we have measured: 1. the fraction of nuclei with a telomeric disk; 2. the fraction of cells in mitosis; and 3. the fraction of cells with interphase nuclei but without a telomeric disk. Ninety percent of the cells formed a telomeric disk 3.5 hours after BrdU incorporation and were therefore interpreted as cells in the late G2 phase (black line and circles). Cells entering mitosis (dashed line and squares) peaked at 7.5 hours (65%) and cells in G1 (dotted line and triangles) peaked after 8.5 hours (57%). The increase in the number of metaphases at 9.5 hours cannot be explained and probably lies within the limits of experimental errors.

compared the telomere distribution volume and shape with that of the 4'-6-Diamidino-2-phenylindole (DAPI) – stained nucleus, and verified that the nucleus itself still had a spherical-like volume. We rarely found distorted nuclei and excluded these cells from the analysis. The nucleus shown in G2 is not fully spherical. Such a shape is expected, because when the telomeres forms a disk, it pools the chromosomes and forces them to be closer to the disk, which results in an oblate shape as well.

To further study the phase transition timing along the cell cycle we used the synchronous bromodeoxyuridine (BrdU) sorting method. The cell population was pulse-labelled with BrdU in the S phase and flow sorted. Cells were placed back into culture and sub-populations harvested at 3.5, 4, 5, 6, 7, 8, 8.5, 9 and 10 hours after labelling and sorting. The cells were then fixed for 3D analysis. A minimum of 20 cells from each of these sub-populations were measured, analyzed and divided into the following three categories: 1) nuclei with a telomeric disk; 2) cells in mitosis; 3) cells in interphase without telomeric disk and mitotic figures (evaluated as G1 cells). The cell fractions as a function of time are shown in Fig. 6. Most cells (90%) form a telomeric disk 3.5 hours after BrdU incorporation. These cells are, therefore, interpreted as cells in the G2 phase. The fraction of metaphase cells peaks at 7.5 hours (65%) and the cell fraction of interphase cells that does not have a telomeric disk (and is interpreted as being in the G1 phase) peaks at 8.5 hours (57%).

These results reveal that the telomeric disk is formed in the late G2 phase. As cells progress from G2 to M, chromosomes organize into metaphases and, therefore, the number of cells in interphase with a telomeric disk decreases. Because there is no other state of transition between telomeric disk and mitosis, we conclude that the telomeric disk is the 3D telomeric organization assumed in late G2. Thus, it is also the final stage of the interphase nucleus that permits the organization of the genetic material prior to its entry into the M phase and prior to chromosome segregation. Cells in late G2 with a telomeric disk have additional characteristic features: i) they exhibit a larger overall nuclear volume than their G1 or S phase counterparts (this increase in size was also confirmed by fluorescent activated cell sorter [FACS] analysis); and ii) they begin to show signs of early re-organization of the chromatin into partially condensed areas (as visualized using the DAPI stained image).

At the end of the M phase, we observe cells that enter into the G1 conformation of telomeres, with a wide spatial distribution of telomeres throughout a smaller nucleus.

In conclusion, this data indicates that the telomeric disk is a novel structure within the interphase nucleus in late G2 that has not been previously described. Its existence points to the fundamental importance of ordered nuclear organization at the end of G2. The telomeric disk probably assures the proper organization of chromosomes prior to mitosis and their organized segregation during mitosis. Together with information that has been previously published on telomeric dynamics [26,28], it is tempting to speculate that telomeres take an active part in the process of chromosome organization into a unique structure, the telomeric disk, during G2. This alignment of telomeres and chromosomes would facilitate the proper subsequent organization of the chromosomes into an equatorial plane during cell division. This process may be driven by the telomeres themselves (that are free of the nuclear matrix) or through the nuclear matrix. The telomeric disk may also allow for a late G2 checkpoint.

Further work on the subject can also be performed *in vivo*, as has been shown by Molenaar *et al.* [26]. In such a way the full dynamic process can be observed, which is complementary to the single time-points that are shown in our work.

We have continued to observe the distribution of telomeres in cancer cells. Typical 3D images constructed from normal nuclei and from a Burkitt lymphoma cell line (Raji), as well as from primary mouse plasmacytoma (PCT) and primary human head and neck squamous cell carcinoma (HNSCC) stage IV (Fig. 7), show that telomeres form aggregates and thus a partially altered telomeric disk. Such telomeric aggregates are characterized by both a larger volume and larger integrated intensity than their normal non-overlapping and non-aggregated counterparts. They are not observed in normal cells. Similar results for altered telomeric organization have also been found in human neuroblastoma and colon carcinoma tumor cell lines.

In line with these concepts, oncogenic activation remodels this nuclear order and sets the stage for genomic instability as we have recently measured for conditional c-Myc deregulation. We have found that deregulated expression of c-Myc alters the 3D nuclear organization of chromosomes and telomeres, and makes genomic rearrangements topologically feasible (Chuang *et al.*, in preparation).

## Conclusions

In summary, we have shown that 3D optical imaging followed by the analysis of telomeres in the interphase is an important tool for basic research and cancer biology. We have found cell-cycle dependence of the telomere organization in the nucleus, where telomeres align into a telomeric disk during the late G2 phase. Such an organization has never before been reported.

Telomeric aggregates are found in tumor cells and, therefore, an alteration of the telomeric disk is seen. Transient telomeric aggregations potentially cause irreversible chromosomal rearrangements.

The above findings indicate that it is now possible to examine the presence of telomeric aggregates suggestive of genomic instability in individual interphase nuclei and tissue, without the need to examine metaphases. Such new directions of monitoring genomic instability could potentially have an impact on cancer biology, genetics, diagnostic innovations and surveillance of treatment response in medicine.

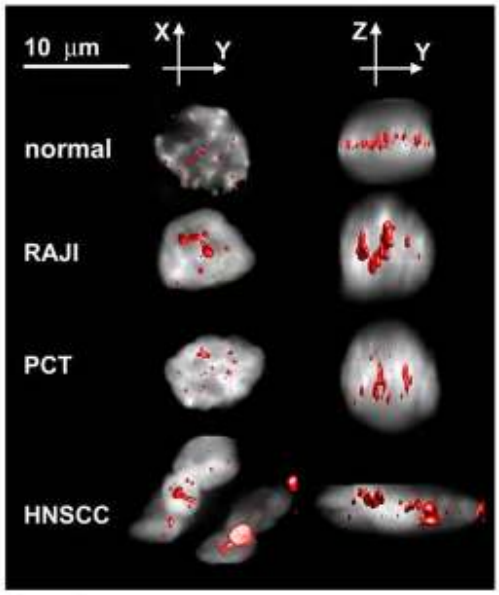


**Figure 7**
Normal: A normal blood cell; RAJI: A Burkitt lymphoma cell line; PCT: A primary mouse plasmacytoma cell; HNSCC: A primary human head and neck squamous cell carcinoma (stage IV). The distribution of telomeres in cancer cells compared with a normal cell. Images are shown as explained in Fig. 5. Aggregates of telomeres are formed and the telomere disk that appears in the G2 phase is distorted.

## Methods

### *Cells*

Mouse primary cells were directly isolated from BALB/c mice and stimulated with lipopolysaccharide to enter into the cell cycle [29]. Primary mouse fetal liver cells were also directly isolated from BALB/c mice. Mice were studied according to the protocols approved by Canadian Central Animal Care. Immortalized mouse pro B lymphocytes have been described elsewhere [30]. Human primary cells were obtained from healthy donors. Head and neck squamous cell carcinoma and control tissue were obtained from a patient at CancerCare Manitoba upon ethics approval and informed consent.

### *Fixation techniques*

Pro B lymphocytes [30] were fixed in four ways: i) following cytospin preparations, cells were fixed in 3.7% formaldehyde (1×PBS/50 mM $MgCl_2$); ii) cells were allowed to

grow on glass slides and were fixed in 1% formaldehyde (3D fixation); iii) cells were fixed in suspension with 3.7% formaldehyde (3D fixation); and iv) cells were fixed in methanol:acetic acid (3:1) according to standard protocols [29]. Tissue was fixed following cryosection (5 μm sections were used) in 1% formaldehyde (1×PBS/50 mM $MgCl_2$). All hybridizations shown in this report were carried out after 3D fixation.

#### *Fluorescent activated cell sorter (FACS) analysis*

For FACS analysis, primary lymphocytes were fixed in 70% cold ethanol and stained with propidium iodide (1 μg/mL) following RNAse (20 μg/mL) digestion. The stained cells were analysed for DNA content by flow cytometry in a EPICS Altra cytometer (Beckman-Coulter). Cell cycle fractions were quantified with WinCycle software (Phoenix Flow Systems, San Diego, CA).

#### *Cell sorting*

Cells were stained with Hoechst 33342 (Molecular Probes) at a final concentration of 1 μg/mL for 90 minutes at 37°C and 5% of carbon dioxide ($CO_2$). Cells were sorted according to their DNA content (G0/G1, S and G2/M phases) with a EPICS Altra cytometer (Beckman-Coulter) equipped with a UV laser (Coherent, excitation at 350 nm) and a 460 nm band-pass filter.

#### *BrdU labelling*

Pro B lymphocytes were labelled *in vivo* with 10 μM of BrdU (5-Bromo-2'-deoxyuridine, SIGMA-ALDRICHT, Lyon, France) for one hour at 37°C in humidified atmosphere (5% $CO_2$). BrdU was then detected with 5 μL/1×106 cells of anti-BrdU-FITC (fluorescein isothiocyanate) antibody (TEBU, Le Perray-en-Yvelines, France) at identical conditions for 30 minutes. Thereafter, all BrdU (i.e. FITC)-positive cells were live sorted, placed into culture for different times and harvested at 3.5, 4, 5, 6, 7, 8, 8.5, 9 and 10 hours after labeling and sorting. The cells were then fixed for 3D analysis. For each time point we have measured: 1. the fraction of nuclei with a telomeric disk; 2. the fraction of cells in mitosis; and 3. the fraction of cells in interphase nuclei without telomeric disk and mitotic figures that were evaluated as G1 and S phase cells.

#### *Telomere FISH using Cy3-labled PNA probes*

Telomere FISH was performed as described [31] using a Cy3-labelled PNA probe (DAKO, Glostrup, Denmark). Telomere hybridizations were specific as shown by metaphase hybridizations and the correct number of the telomeric signals observed at the ends of chromosomes prepared from primary cells (Fig. 4).

#### *3D image acquisition*

Unless stated otherwise, 20–30 cells were analyzed by 3D imaging from each cell type and phase type. Part of the measurements were done with a confocal microscope (Leica AOBS-SP) and most of them with a conventional Axioplan 2 (Zeiss) with a cooled AxioCam HR CCD followed by deconvolution [30]. DAPI, FITC and Cy3 filters (Zeiss) were used in combination with Planapo 63×/1.4 oil (Zeiss). Axiovision 3.1 software with a deconvolution module and rendering module were used (Zeiss). Both methods gave similar results.

80–100 sections were acquired for each 3D nucleus, typically with 200 × 200 pixels per section with a ~100 × 100 nm nominal imaging area per pixel (steps of 200 nm along *Z*). The point-spread function of our system has a full width at half max of approximately 200 nm in the plane and 400 nm along the optical axis.

#### *3D analysis of telomeres*

In order to analyze the telomere distribution in the nucleus, we developed a special 3D image analysis programme. The main algorithmic part is described below. The programme (TeloView) is based on the Matlab computer language (The MathWorks, Natick, MA, USA) and some of the image processing algorithms are based on the DipImage library (developed at the Quantitative Imaging Group, Delft University of Technology, Delft, The Netherlands) [32].

The programme segments the nucleus volume by a derivative-based algorithm using a morphological top and bottom-hat algorithm [33]. The volume, intensity and centre of gravity are calculated for each spot. The programme then finds a principle plane in the nucleus ($x'y'$) that is the closest to all the telomeres (Fig. 2). This is especially important when a tissue section is analyzed, because this plane should not necessarily be parallel to the microscope slide plane.

The telomeric distribution inside the nucleus is described by fitting an ellipsoid to the volume occupied by the telomeres (three different main axes; Fig. 2). The distributions were found to be either oblate or spherical (i.e. the two principle axes along the main $x'y'$ plane of the spheroid are similar). It is, therefore, convenient to describe the distribution volume as a spheroid (i.e. an ellipsoid having two axes of equal length). As such, it is simpler to describe the spheroid degree of variation from a perfect sphere by the ratio $a/c$ where $a$ and $b$ are the similar semi-axes and $c$ is the third one. Such a description reflects the degree to which the telomere's volume is oblate.

## Authors' contributions

TCYC performed the data analysis, wrote the discussion, performed the hybridizations, took all head and neck cancer samples from tumor collections during surgery to preparation of frozen sections, hybridization, analyses

and patient records. SMo performed some of the hybridizations and analyses while visiting SM's lab. YG developed the 3D analysis methods, 3D algorithms and the programme that analyses the nuclei, wrote the paper in its current version and acts as corresponding author. AYCC organized the data, tables, and G2 phase data. ITY, BV and RD took part in the development of the 3D analysis methods and algorithms, and the programme that analyses the nuclei. VM did the BrdU-labelling experiments and G2 study in France and in SM's lab. MP performed the G2 analysis in SM's lab. MB performed the metaphase telomere FISH. PDK directs the programme of head and neck surgery and provided some of the samples that were used for the study. TF supervised VM and MP in France. PB supervised SMo in Heidelberg. SM planned and carried out the project that was performed in SM's lab, and was supervisor for TCYC, SMo (while visiting SM's lab), AYCC, MB, MP and VM, and performed part of the experiments.

## Acknowledgements

The authors wish to thank our colleagues and lab members for discussions and critical reading of this manuscript. This work was supported by the Canada Foundation for Innovation, the Canadian Institutes of Health Research (NSERC), CancerCare Manitoba, Fondation de France (Paris), the French Minister of Foreign Affairs, Sander-Stiftung and Verein zur Förderung der Krebsforschung e.V.

This work was also supported by the Physics for Technology programme of the Foundation for Fundamental Research in Matter (FOM), the Delft Incer-Faculty Research Center Life Tech and the Delft Research programme Life Science and Technology.

## References

1. Pienta KJ, Partin AW, Coffey DS: **Cancer as a disease of DNA organization and dynamic cell structure.** *Cancer Research* 1989, **49**:2525-2532.
2. Cremer C, Cremer Thomas: **Chromosome territories, nuclear architecture and gene regulation in mammalian cells.** *Nature reviews Genetics* 2001, **2**:292-301.
3. Rabl C: **Über Zellteilung.** *Morphologisches Jahrbuch Gegenbaur C (ed)* 1885, **10**:214-330.
4. Marshall WF: **Order and Disorder in the Nucleus.** *Curr Biol* 2003, **12**:R185–R192.
5. Nagele R, Freeman T, McMorrow L, Lee H-y: **Precise spatial positioning of chromosomes during prometaphase: evidence for chromosomal order.** *Science* 1995, **270**:1831-1835.
6. Parada LA, Misteli T: **Chromosome positioning in the interphase nucleus.** *Trends in Cell Biology* 2002, **12**:425-432.
7. Tanabe H, Müller S, Neusser M, von Hase J, Calcagno E, Cremer M, Solovei I, Cremer C, Cremer T: **Evolutionary conservation of chromosome territory arrangements in cell nuclei from higher primates.** *Proc Nat Acad Sci USA* 2002, **99**:4424–4429.
8. Gerlich D, Beaudouin J, Kalbfuss B, Daigle N, Eils R, Ellenberg J: **Global chromosome positions are transmitted through mitosis in mammalian cells.** *Cell* 2003, **112**:751-764.
9. Abney JR, Cutler B, Fillback ML, Axelrod D, Scalettar BA: **Chromatin dynamics in interphase nuclei and its implication for nuclear structure.** *The Journal of Cell Biology* 1997, **137**:1459-1468.
10. Holley WR, Mian IS, Park SJ, Rydberg B, Chatterjee A: **A model for interphase chromosomes and evaluation of radiation-induced aberrations.** *Radiation Research* 2002, **158**:568-580.
11. Cerda MC, Berrios S, Fernandez-Donoso R, Garagna S, Redi C: **Organisation of complex nuclear domains in somatic mouse cells.** *Biology of the Cell* 1999, **91**:55-65.
12. Cornforth Michael N., Greulich-Bode Karin M., Loucas Bradford D., Arsuaga Javier, Vazquez Mariel, Sachs Rainer K., Bruckner Martina, Molls Michael, Hahnfeldt Philip, Hlatky Lynn, Brenner David J.: **Chromosomes are predominantly located randomly with respect to each other in interphase human cells.** *J Cell Biol* 2002, **159**:237-244.
13. Vourc'h Claire, Taruscio Domenica, Boyle Ann L., Ward David C.: **Cell cycle-dependent distribution of telomeres, centromeres, and chromosome-specific subsatellite domains in the interphase nucleus of mouse lymphocytes.** *Experimental Cell Research* 1993, **205**:142-151.
14. Lopez-Velazquez G, Marquez J, Ubaldo E, Corkidi G, Echeverria O, Vazquez Nin GH: **Three-dimensional analysis of the arrangement of compact chromatin in the nucleus of G0 rat lymphocytes.** *Histochemistry and Cell Biology* 1996, **105**:153-161.
15. Dong F, Jiang J: **Non-Rabl patterns of centromere and telomere distribution in the interphase nuclei of plant cells.** *Chromosome Research* 1998, **6**:551-558.
16. Ferguson M, Ward DC: **Cell cycle dependent chromosomal movement in pre-mitotic human T-lymphocyte nuclei.** *Chromosoma* 1992, **101**:557-565.
17. Gasser SM: **Visualizing chromatin dynamics in interphase nuclei.** *Science* 2002, **296**:1412-1416.
18. McClintock Barbara: **The stability of broken ends of chromosomes in Zea Mays.** *Genetics* 1941, **26**:234-282.
19. Blackburn EH: **Switching and signaling at the telomere.** *Cell* 2001, **106**:661-673.
20. Maser RS, DePinho RA: **Connecting chromosomes, crisis, and cancer.** *Science* 2002, **297**:565-569.
21. Cremer T, Cremer C, Baumann H, Luedtke EK, Sperling K, Teuber V, Zorn C: **Rabl's model of the interphase chromosome arrangement tested in Chinese hamster cells by premature chromosome condensation and laser-UV-microbeam experiments.** *Human Genetics* 1982, **60**:46-56.
22. Zalensky AO, Allen MJ, Kobayashi A, Zalenskaya IA, Balhorn R, Bradbury EM: **Well-defined genome architecture in the human sperm nucleus.** *Chromosoma* 1995, **103**:577-590.
23. Weierich Claudia, Brero Alessandro, Stein Stefan, Hase Johann von, Cremer Christoph, Cremer Thomas, Solovei Irina: **Three-dimensional arrangements of centromeres and telomeres in nuclei of human and murine lymphocytes.** *Chromosome Research* 2003, **11**:485-502.
24. Armstrong SJ, Franklin FCH, Jones GH: **Nucleolus-associated telomere clustering and pairing precede meiotic chromosome synapsis in Arabidopsis thaliana.** *Journal of Cell Science* 2001, **114**:4207-4217.
25. de Lange T: **Human telomeres are attached to the nuclear matrix.** *The EMBO Journal* 1992, **11**:717-724.
26. Molenaar C, Wiesmeijer K, Verwoerd NP, Khazen S, Eils R, Tanke HJ, Dirks RW: **Visualizing telomere dynamics in living mammalian cells using PNA probes.** *The EMBO Journal* 2003, **22**:6631-6641.
27. Barber C. Bradford, Dobkin P. David, Huhdanpaa Hannu: **The quickhull algorithm for convex hulls.** *ACM Transactions on Mathematical Software* 1996, **22**:469–483.
28. Nagele Robert G., Velasco Antonio Q., Anderson William J., McMahon Donald J., Thomson Zabrina, Fazekas Jessica, Wind Kelly, Lee Hsin-yi: **Telomere associations in interphase nuclei: possible role in maintenance of interphase chromosome topology.** *Journal of Cell Science* 2001, **114**:377-388.
29. Beatty B, Mai S, Squire J: **FISH: A practical Approach.** Oxford University Press, USA.; 2002:274.
30. Fest T, Mougey V, Dalstein V, Hagerty M, Milette D, Silva S, Mai S: **c-MYC overexpression in Ba/F3 cells simultaneously elicits genomic instability and apoptosis.** *Oncogene* 2002, **21**:2981-2990.
31. Figueroa R, Lindenmaier H, Hergenhahn M, Nielsen KV, Boukamp P: **Telomere erosion varies during in vitro aging of normal human fibroblasts from young and adult donors.** *Cancer Research* 2000, **60**:2770-2774.
32. **DIPimage, a scientific image processing toolbox for MATLAB** [http://www.ph.tn.tudelft.nl/DIPlib/]
33. Meyer Fernand: **Iterative image transformations for an automatic screening of cervical smears.** *The Journal of Histochemistry and Cytochemistry* 1979, **27**:128-135.

## 2.2 *c-Myc* induces chromosomal rearrangements through telomere and chromosome remodeling in the interphase nucleus.

Access the publication online is available via the following link:

http://www.pnas.org/content/102/27/9613.long

**Rationale of investigation**

*c-Myc* is a proto-oncogene found in more than 70% of human cancers. Telomere aggregation and dysfunction are frequently observed in tumor cells as described in my paper "The three-dimensional organization of telomeres in the nucleus of mammalian cells" (Chuang et al 2004). One of the mechanisms of telomere dysfunction is mediated by *c-Myc* deregulation.

**Objectives**

To investigate the effect of conditional over-expression of *c-Myc* on telomeres, quantitative 3-D analysis of telomeres is carried out via deconvolution microscopy and the Teloview software. Upon deregulation of *c-Myc*, spectral karyotyping was carried out to assess chromosomal aberrations.

**Hypothesis**

Deregulation of *c-Myc* first leads to telomeric dysfunction including aggregation and fusion, which will lead to breakage-bridge-fusion process that causes chromosomal aberration.

**Summary of findings**

Conditional *c-Myc* induction disrupts 3D telomere organization by forming cycles of telomeric aggregates in interphase nuclei. These cycles lead to the onset of genomic instability as demonstrated by the breakage-bridge-fusion

(BBF) cycles that results in nonreciprocal translocations and chromosomal rearrangement. In addition, telomere fusions were observed on metaphases.

**My contribution**

I conceived the project idea in collaboration with Dr. Sabine Mai and Dr. Alice Chuang to investigate *c-Myc* deregulation as a mechanism of telomere dysfunction. I performed 3-D telomere FISH, 3-D image acquisition and analysis of images. The work contributed to figures 1, 2, and 3. I was involved in manuscript preparation, writing, revision and submission to various publishers.

PNAS

# c-Myc induces chromosomal rearrangements through telomere and chromosome remodeling in the interphase nucleus

Sherif F. Louis*†, Bart J. Vermolen†‡, Yuval Garini†‡, Ian T. Young§, Amanda Guffei*, Zelda Lichtensztejn*, Fabien Kuttler*, Tony C. Y. Chuang*§¶, Sharareh Moshir*‖, Virginie Mougey**, Alice Y. C. Chuang*, Paul Donald Kerr§, Thierry Fest**††, Petra Boukamp‖, and Sabine Mai*‡‡

*Manitoba Institute of Cell Biology, University of Manitoba, 675 McDermot Avenue, Winnipeg, MB, Canada R3E 0V9; §Department of Imaging Science and Technology, Faculty of Applied Sciences, Quantitative Imaging Group, Delft University of Technology, 2628 CJ Delft, The Netherlands; ¶Department of Otolaryngology Head and Neck Surgery, Health Sciences Centre, GB421-820 Sherbrook Street, Winnipeg, MB, Canada R3A 1R9; ‖Division of Genetics of Skin Carcinogenesis, German Cancer Research Centre, Im Neuenheimer Feld 280, 69120 Heidelberg, Germany; **Hematology Department, IETG Laboratory, University Hospital Jean Minjoz, 25030 Besançon, France; and ††Hematology Department, EA 3889, IFR140 GFAS, University Hospital Pontchaillou, 35033 Rennes, France

Edited by George Klein, Karolinska Institutet, Stockholm, Sweden, and approved May 9, 2005 (received for review October 11, 2004)

**In previous work, we showed that telomeres of normal cells are organized within the 3D space of the interphase nucleus in a nonoverlapping and cell cycle-dependent manner. This order is distorted in tumor cell nuclei where telomeres are found in close association forming aggregates of various numbers and sizes. Here we show that c-Myc overexpression induces telomeric aggregations in the interphase nucleus. Directly proportional to the duration of c-Myc deregulation, we observe three or five cycles of telomeric aggregate formation in interphase nuclei. These cycles reflect the onset and propagation of breakage-bridge-fusion cycles that are initiated by end-to-end telomeric fusions of chromosomes. Subsequent to initial chromosomal breakages, new fusions follow and the breakage-bridge-fusion cycles continue. During this time, nonreciprocal translocations are generated. c-Myc-dependent remodeling of the organization of telomeres thus precedes the onset of genomic instability and subsequently leads to chromosomal rearrangements. Our findings reveal that c-Myc possesses the ability to structurally modify chromosomes through telomeric fusions, thereby reorganizing the genetic information.**

genomic instability | 3D nucleus | breakage-bridge-fusion

Multiple alterations accompany tumor initiation and progression resulting in the modulation of gene expression and in genomic instability. These interconnected changes occur within nuclei that harbor an altered 3D organization (1–3). In agreement with this concept, recent reports suggest tumor-associated changes of chromosomal organization in an altered 3D nucleus (3–8). However, mechanisms leading to structural changes of telomeres and chromosomes remain elusive.

We recently reported that the normal interphase nucleus has a unique 3D telomeric organization that is cell cycle dependent (9, 10). Telomeres are organized in a nonoverlapping manner and align into a central telomeric disk during the late $G_2$ phase of the cell cycle (9). In contrast, tumor cells display an aberrant organization of telomeres that can be objectively measured in nuclei showing telomeric aggregates of various complexity and sizes (9).

Constitutive expression of c-Myc due to chromosomal translocations, mutation, or amplification contributes to the development and progression of many cancers (11, 12). c-Myc deregulation directly promotes genomic instability (13), causing locus-specific and karyotypic instability (14–18). Additionally, c-Myc induces illegitimate replication initiation (19, 20), DNA breakage (21), alterations of DNA repair (22, 23), and a low level of point mutations (24, 25). Effects of c-Myc on genomic instability are reversible after a transient experimental activation of c-Myc (15). However, c-Myc continues to generate instability after constitutive deregulation (16). *In vivo*, c-Myc deregulation directly initiates and promotes tumorigenesis (26–30). When c-Myc deregulation is abolished, *in vivo* tumorigenesis is reversible, provided that no additional mutations had occurred (29–34).

Prompted by the complexity of downstream genetic alterations that result from c-Myc deregulation, we investigated whether c-Myc affected the 3D organization of the mammalian interphase nucleus and whether this remodeling had an impact on genomic stability. We show that c-Myc deregulation causes remodeling of the 3D nuclear organization of telomeres and chromosomes, thus creating the topological conditions that initiate genomic instability.



## Materials and Methods

**Cells and Conditional Myc Activation.** Culture conditions have been described for Ba/F3 (35) and PreB (36) cells. The plasmacytoma cell line MOPC460D was a gift of J. Mushinski (National Institutes of Health, Bethesda). Cell viability was determined by hemocytometer counts by using trypan blue. The primary mouse plasmacytoma DCPC21 was isolated from a BALB/c mouse (37). *v-abl/myc*-induced plasmacytomas (38) and primary lymphocytes were collected from BALB/c mice (Central Animal Care protocol 02-039).

To activate MycER (39) in Ba/F3 or PreB cells, $10^5$ cells per ml were treated with 100 nM 4-hydroxytamoxifen (4HT). Cells were split 24 h before 4HT treatment. Non-4HT treated control cells were cultivated in ethanol, which is used to dissolve 4HT (25, 26, 39). Two different MycER activation schemes were performed. First, analyses of c-Myc-induced changes in 3D telomere organization were carried out after a single addition of 4HT that was left in the culture medium until its biological effects subsided (40–42). Nuclei were examined every 24 h over a 10-day period. A second time course was performed every 6 h for 120 h (Fig. 1). To enable a time-dependent analysis of Myc activation, 4HT was given for 2 or 12 h and was removed. Alternatively, 4HT was added every 12 h or was given once but left in the culture. MycER activation was determined by fluorescent immunohistochemistry.

**Immunohistochemistry (IHC).** Fluorescent IHC of Myc protein was performed as described in ref. 43 by using a polyclonal anti-c-Myc antibody (N262; Santa Cruz Biotechnology) and a goat anti-rabbit IgG FITC antibody, each at a dilution of 1:100. Analysis was

This paper was submitted directly (Track II) to the PNAS office.

Abbreviations: 4HT, 4-hydroxytamoxifen; SKY, spectral karyotyping; TA, telomeric aggregate.

†S.F.L., B.J.V., and Y.G. contributed equally to this work.

‖Present address: Department of Otolaryngology Head and Neck Surgery, Head and Neck Division, The Johns Hopkins University School of Medicine, Baltimore, MD 21205.

‡‡To whom correspondence should be addressed. E-mail: smai@cc.umanitoba.ca.

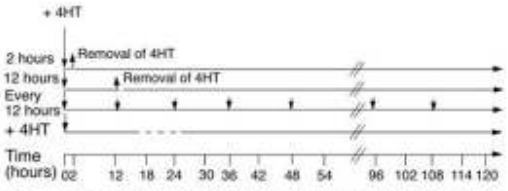


**Fig. 1.** MycER activation scheme. The effects of 4HT last 15–24 h in cell lines (40–42), as indicated by dashed lines. Cells were harvested every 6 h over a time period of 120 h. Mock-treated control cells were processed in parallel.

performed by using a Zeiss Axiophot 2 microscope. Images were acquired with a Cooke CCD SensiCam Camera.

**Cell Death.** Apoptotic bodies for control and MycER-activated cells were assessed by two independent observers who scored 300 DAPI-stained nuclei per time point in the presence or absence of MycER activation.

**Telomere FISH.** Ba/F3, PreB, and plasmacytoma cells were collected (200 × *g* for 10 min) and resuspended in PBS containing 3.7% formaldehyde (Fluka) and incubated for 20 min. Thereafter, the telomere FISH protocol was performed (9, 44) by using Cy3- or FITC-labeled PNA probes (DAKO). Three independent experiments were performed. At least 30 nuclei and 20 metaphases were examined per time point. Imaging of metaphases after telomere FISH was performed by using Zeiss Axioplan 2 with a cooled AxioCam HR B&W, DAPI, Cy3, or FITC filters in combination with Planapo 63x/1.4 oil objective lens. Images were acquired by using AXIOVISION 3.1 (Zeiss) in multichannel mode. Because of the presence of multiple variables, the general linear modeling procedure was used. To test average aggregates among different groups, a two-way ANOVA test was performed for normality and robustness of the data. For details of all tests preformed, see *Supporting Materials and Methods*, which is published as supporting information on the PNAS web site.

**3D Image Acquisition.** At least 30 nuclei were analyzed for each time point. AXIOVISION 3.1 with deconvolution module and rendering module were used. For every fluorochrome, the 3D image consists of a stack of 100 images with a sampling distance of 200 nm along the *z* and 107 nm in the *xy* direction. The constrained iterative algorithm option was used (45).

**3D Image Analysis for Telomeres.** Telomere measurements were done with TELOVIEW (9, 46). By choosing a simple threshold for the telomeres, a binary image is found. Based on that, the center of gravity of intensities is calculated for every object resulting in a set of coordinates (*x*, *y*, *z*) denoted by crosses on the screen. The integrated intensity of each telomere is calculated because it is proportional to the telomere length (47). The integration region is determined by growing a sphere on top of the found coordinate. After every step of growth (iteration), the sum under this volume (the telomere) is subtracted by the sum just surrounding it (background level). When the process of the growth of the sphere does not contribute to an integrated intensity increase, the algorithm stops and the integrated intensity of the telomere with an automatic background correction is obtained.

**Chromosome Painting and Measurements of Chromosomal Overlap(s) in Interphase Nuclei.** Chromosome painting was carried out as described in ref. 48 by using paints for mouse chromosomes 5 (Cy3), 13 (FITC), 7 (Cy3), 10 (FITC), and 17 (FITC) from Applied Spectral Imaging (Vista, CA). 3D image acquisition of painted nuclei was performed as described above. Measurements of chromosomal overlaps were performed after 3D image acquisition and constrained iterative deconvolution as follows: (*i*) based on the DAPI counterstain image, we determined the 3D boundary of the nuclear volume. Data outside that volume were ignored. (*ii*) For each one of the chromosomes, we determined an intensity threshold and referred only to voxels that were above the threshold that belonged to the specific chromosomes. The total volume occupied by each one of the chromosome pairs is measured ($V_1$ and $V_2$). (*iii*) The volume occupied by both chromosome pairs is measured, $V_o$. By dividing this value by $V_1$ and by $V_2$, the level of overlap relative to the total volume of each chromosome pair was measured, $V_o/V_1$, $V_o/V_2$ (for details, see Fig. 8 which is published as supporting information on the PNAS web site).

**Spectral Karyotyping (SKY).** Mouse SKY was performed by using a SKY system (Applied Spectral Imaging) (37). Twenty metaphases were examined per time point. Significant values for chromosomal rearrangements were determined after MycER activation. Mean total chromosomes and numbers of each chromosome observed for control and Myc-activated cells were compared over time by two-way ANOVA. In addition, statistical analyses were performed for the occurrence of translocations, breakages, and fusions over the experimental period of 120 h. $P$ values of $<0.05$ were considered significant. Only the frequency procedure was used, followed by Fisher's exact test. The $P$ value of the overall study was $<0.0001$.

**Supporting Information.** For additional information, see Figs. 9–12, Movies 1–3, and Tables 2–4, which are published as supporting information on the PNAS web site.

## Results

**The 3D Organization of Telomeres Before c-Myc Activation.** We examined whether c-Myc deregulation affected the 3D organization of telomeres in the interphase nucleus. To this end, we analyzed the effect of conditional c-Myc expression in two independent immortalized mouse B lymphocyte lines, Ba/F3 (35) and PreB (36), stably transfected with MycER (39). For both cell lines, we first evaluated the 3D organization of telomeres in nuclei of non-MycER-activated cells by using primary BALB/c B lymphocytes as a control. Consistent with our previous studies (9), telomeres of normal primary BALB/c B nuclei showed nonoverlapping telomere posi-

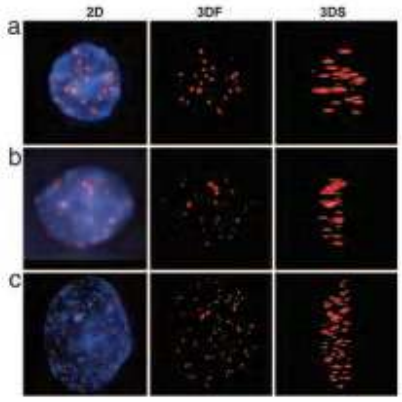


**Fig. 2.** Telomeric organization in interphase nuclei of primary and immortalized B lymphocytes without overlap in telomere positions. (*a*) Primary B cell nucleus. (*b*) Nucleus of near diploid PreB cell. (*c*) Nucleus of tetraploid Ba/F3 cell. Telomeres are shown in red; nuclei in blue. 3DF, 3D front view; 3DS, 3D side view.

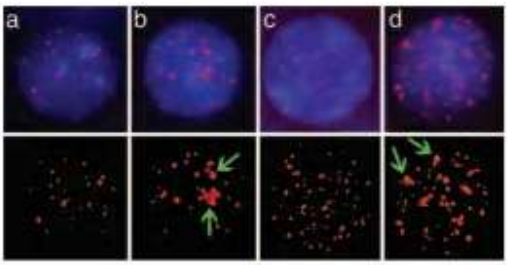


Fig. 3. c-Myc deregulation induces TAs in interphase nuclei of PreB and Ba/F3 cells shown at 72 h after 4HT-treatment. (*a*) Mock-treated PreB cells show nonoverlapping telomeres (red). (*b*) MycER-activated PreB cells with TAs (green arrow). (*c*) Mock-treated Ba/F3 cells show nonoverlapping telomeres. (*d*) MycER-activated Ba/F3 cells show the formation of TAs (green arrow).

tions as determined by 3D imaging (Fig. 2*a*). Without MycER activation, both PreB and Ba/F3 interphase nuclei also displayed nonoverlapping telomere positions (Fig. 2 *b* and *c*, respectively). Therefore, the above cell lines were appropriate to study the effects of conditional c-Myc activation on the 3D telomeric organization.

**c-Myc-Dependent Disruption of the 3D Telomeric Organization: Formation of Telomeric Aggregates (TAs) in Interphase Nuclei.** We next analyzed the effect of conditional c-Myc expression on the 3D organization of telomeres. After a transient MycER activation with 4HT, nuclear c-Myc signals were observed in both PreB and Ba/F3 cells (Fig. 9 *b* and *d*). In non-4HT treated control cells, MycER was found in the cytoplasm (Fig. 9 *a* and *c*; see also ref. 39).

To determine whether c-Myc deregulation affected the 3D organization of telomeres, we performed time course experiments. In the first set of experiments, c-Myc deregulation and 3D telomeric organization were investigated in both PreB and Ba/F3 cells after a single 4HT treatment. Nuclei were analyzed after c-Myc deregulation at 0, 24, 48, 72, and 96 h and at 10 days and compared with nuclei from mock-treated control cells. In both cell lines, analyses of the 3D nuclear organization of telomeres revealed that c-Myc deregulation induced the formation of TAs. TAs are group(s) of telomeres that are found in clusters and, thus, in close association in the interphase nucleus. This 3D telomeric organization is distinct from the normal 3D organization of non-MycER-activated PreB, Ba/F3 cells and primary mouse lymphocytes (Fig. 2). Fig. 3 illustrates the presence of TAs in interphase nuclei of MycER-activated PreB and Ba/F3 cells (Fig. 3 *b* and *d*, respectively). Although such TAs had been observed in tumor cell nuclei previously (9), their presence in conditional c-Myc expressing cells is a previously uncharacterized finding.

**c-Myc Induces Cycles of TAs in Interphase Nuclei.** In subsequent experiments, we investigated the time relationship between c-Myc deregulation and the formation of TAs more closely. To this end, cells were harvested every 6 h over a time period of 120 h. We also varied the duration of conditional c-Myc expression (Fig. 1), confirming nuclear c-Myc staining as above (Fig. 9 and 11). Next, the 3D organization of telomeres was determined (Fig. 4). At this point, we focused on near diploid PreB cells only (49). Our positive controls were cells constitutively overexpressing c-Myc [mouse plasmacytomas (27) and a plasmacytoma line (Fig. 4*Ae*)]. Negative controls were mock-treated PreB cells (Fig. 4*Aa*).

This time course confirmed that c-Myc deregulation induced TAs. Representative images show that TAs varied in size and numbers per MycER-activated PreB cell nucleus (Fig. 4*A b–d*, red arrows). High induction levels of TAs were observed at 30, 48, 72, and 96 h declining after 96 h (Fig. 4*B*, arrows). The highest levels

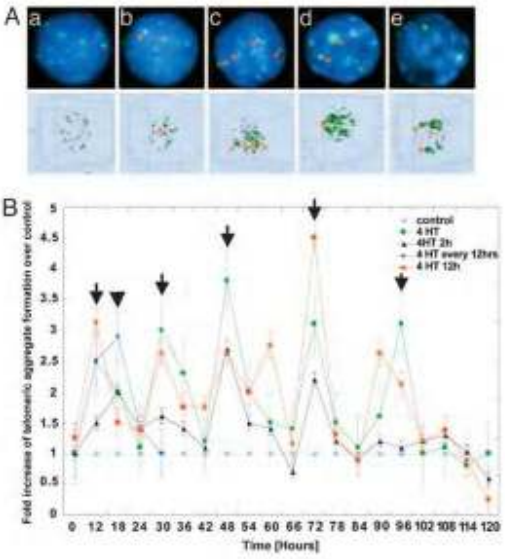


Fig. 4. c-Myc-induced telomeric aggregates appear in cycles. (*A*) Conditional c-Myc deregulation causes TA formation. (*Aa*) Negative control: non-Myc-deregulated PreB nucleus with nonoverlapping 3D telomeric nuclear positions. (*Ab–Ad*) TAs of various sizes and numbers are present after conditional c-Myc expression at any given time point of TA formation. Telomeres are shown in green; TAs by red arrows. (*Ae*) Positive control: plasmacytoma cell line, MOPC460D, with constitutive c-Myc deregulation due to T12;15, shows TAs. Similar results were obtained with primary plasmacytoma cells (data not shown). (*B*) c-Myc induces cycles of TAs. Fold increase in TAs over control levels during a period of 120 h. During this period, c-Myc had been up-regulated for different lengths of time (see Fig. 1). Black, 4HT given for 2 h and removed; red, 4HT administered for 12 h and removed; green, 4HT added once and not removed; blue, 4HT added at 0, 12, and 24 h; gray, control cells. The highest levels of TA formation and a single TA peak observed after consecutive activations of MycER are shown by arrows and an arrowhead, respectively. Error bars represent a 95% confidence interval of binomial distributions.

of TA formation will hereafter be referred to as peaks of TAs. The 6-h time course performed over 120 h indicated that TAs formed in a c-Myc-dependent manner and showed a cyclic appearance (Fig. 4*B*). The number of TA cycles was directly linked to the duration of c-Myc deregulation. For example, 2 h of Myc activation induced three such cycles, whereas 12 h led to five cycles (Fig. 4*B*, black and red lines, respectively). 4HT, left in the culture medium until its biological effects on our cells subsided (Fig. 1), also induced five TA cycles (Fig. 4*B*, green line). In this context, repeated consecutive activations of MycER given every 12 h caused TAs in 96% of all nuclei. These cells died after 30 h (Fig. 4*B*, blue line) because of repeated cycles of c-Myc deregulation and not due to toxicity exerted by 4HT (50). Thus, only a single TA cycle is observed in this experimental setting (Fig. 4*B*, arrowhead). The increase in TAs and 3D volumes was significant (Table 3).

**The c-Myc-Induced TA Cycles Represent Breakage-Bridge-Fusion (BBF) Cycles and Chromosomal Rearrangements.** The cycles of c-Myc induced TAs in PreB nuclei showed similar periodicity for all c-Myc activation periods (Fig. 4*B*). We reasoned that these cycles might reflect both ongoing associations and dissociations of telomeres or BBF cycles. The BBF cycle could be induced by the breakage of dicentric chromosomes during anaphase-inducing apoptosis of cells

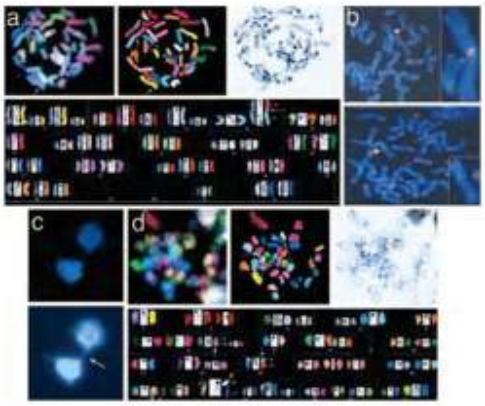


**Fig. 5.** Molecular cytogenetic evidence of BBF cycles in MycER-activated PreB cells. (*a*) SKY analysis reveals telomeric fusions and chromosome breakage. (*a Upper*) Metaphase, raw image (*Left*); metaphase, classified image (*Center*); and metaphase, inverted DAPI image (*Right*). (*a Lower*) Spectral karyotype. End-to-end fusion of chromosomes 18 and 4 (red arrow) and fusion of chromosome 1 with a broken piece of chromosome 1 (green arrow) are shown. One broken chromosome 1 is circled. Note additional broken chromosomes 1, 2, 3, and 7. (*b*) End-to-end fusions of chromosomes revealed by telomere FISH. (*Upper*) Centromeric fusion (see arrow and insert). (*Lower*) Telomeric fusion (see arrow and insert). (*c*) Anaphase bridges. (*Upper*) Short exposure of DAPI stained nucleus (100 msec). (*Lower*) Longer exposure (500 msec) of same image makes anaphase bridge visible (white arrow) but overexposes nuclei. (*d*) SKY illustrating chromosomal fusions (red arrow) and nonreciprocal translocations (white arrows). Broken chromosomes are also present (chromosomes 4, 6, 12, and 17).

having multiple or large TAs per nucleus. To address these possibilities, we first examined metaphase chromosomes at different times: prior, during, and after the peaks of TA formation for a 120-h period. We used both whole-genome analysis by mouse SKY and telomeric FISH of metaphase chromosomes. A significant level of dicentric chromosomes was noted (Fig. 5). Control cells had normal karyotypes (Fig. 12). In MycER-activated PreB cells, however, fusions had occurred. We show as example fusions at the telomeric ends of chromosomes 18 and 4 (Fig. 5*a*), red and green arrows) and between two chromosomes 1 (Fig. 5*a*, green arrow). Chromosome 1 was probably broken in the previous anaphase (Fig. 5*a*, green circle). An additional terminally deleted chromosome 1 is in the center of the same metaphase plate, and chromosomes 2, 3, and 7 reveal terminal deletions (Fig. 5*a*). Telomeric fusions involving both ends of chromosomes as well as sister chromatids were confirmed by telomeric FISH (Fig. 5*b*). Anaphase bridges and ring chromosomes were present (Fig. 5*c*) and data not shown).

**Table 1. Apoptosis levels in non-MycER and MycER-activated PreB cells**

| Time, h | % apoptosis: Controls | % apoptosis: MycER-activated PreB cells | Fold Increase |
|---|---|---|---|
| 0 | 3.0 | 3.0 | 1.0 |
| 12 | 2.0 | 4.0 | 2.0 |
| 24 | 6.0 | 12.0 | 2.0 |
| 30 | 4.0 | 10.0 | 2.5 |
| 42 | 2.0 | 8.0 | 4.0 |
| 48 | 5.0 | 10.0 | 2.0 |
| 66 | 4.0 | 11.0 | 2.75 |
| 72 | 3.0 | 8.0 | 2.7 |
| 84 | 3.0 | 5.0 | 1.7 |
| 96 | 3.0 | 3.0 | 1.0 |
| 102 | 2.0 | 3.0 | 1.5 |

The nature of c-Myc-induced 3D structural changes in interphase nuclei of conditionally Myc expressing cells was as follows: at peaks of TA formation and thereafter, a significant increase in end-to-end chromosomal fusions over control levels was observed. This result was followed by a significant increase in broken chromosomes and nonreciprocal translocations (Figs. 5*d* and 6 and Table 2). In conclusion, TA cycles unveil BBF cycles, namely the fusions of two chromosomes, consequently, the formation of dicentrics and their subsequent breakage in anaphase (Fig. 5). The cycles are induced by conditional Myc deregulation and lead to the onset of genomic instability, demonstrated by the chromosomal rearrangements resulting from these BBF cycles (Figs. 5 and 6 and Table 2).

Next, we investigated whether cells with TAs died during the course of the experiments. If this possibility was the case, we would expect a correlation of cell death in Myc-activated cells at the peak of TA formation or shortly thereafter. The level of apoptosis was ≈2-fold higher in Myc-activated cells than in control cells (Table 1). There was no preference in apoptotic cell death for any specific time point during the 120 h. We concluded that BBF cycles, not apoptosis, contributed to the cycles of TA formation.

**3D Organization of Chromosomes in c-Myc Activated Interphase Nuclei.** TAs and the initiation of BBF cycles with subsequent chromosomal rearrangements prompted us to investigate whether chromosomes were affected in their 3D nuclear positions during MycER activation. To this end, we examined the overlap of specific chromosomes over the 120-h period. SKY of MycER-activated PreB cells suggested chromosomal rearrangements involving chromosomes 7, 13, and 17. Additional rearrangements were found but

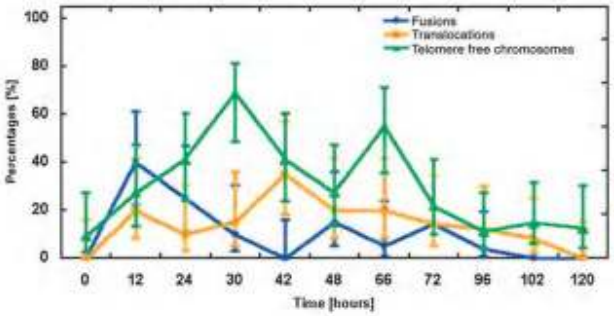


**Fig. 6.** Chromosomal aberrations in MycER-activated PreB cells over a period of 120 h after a single administration of 4HT. End-to-end fusions (blue) increase to 40% in the first 12 h. Over time, the percentage of fusions decreases. Translocations (orange) appear at 12 h and reach a maximum of 35% at 42 h. Telomere-free chromosomal end(s) (green) increase over time peaking at 30 h with 75% of metaphases having at least one telomere-free chromosomal end. Subsequently, the percentage of telomere-free chromosomal end(s) decreases. Q-FISH experiments confirmed healing of telomeric ends at later time points. The error bars show the 95% confidence interval for binomial distributions (51). Because of a confidence interval, the error bars are larger than expected when a standard error would have been used, which was not applicable in this situation. For details on each time point and aberration, see Table 2.

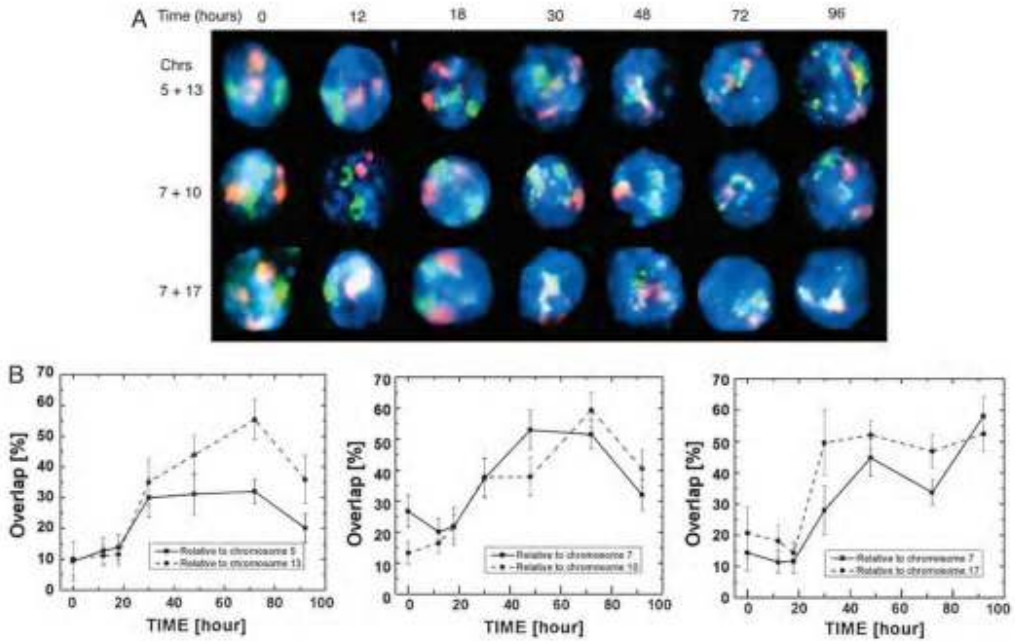


**Fig. 7.** Chromosome positions in Myc-activated nuclei. (*A*) Representative nuclei painted with chromosome paints over a period of 96 h after 4HT (Fig. 1). (*Top*) Chromosomes 5 and 13. (*Middle*) Chromosomes 7 and 10. (*Bottom*) Chromosomes 7 and 17. (*B*) Measurements of chromosomal overlaps in nuclei of c-Myc deregulated cells for chromosomes 5 and 13 (*Left*), 7 and 10 (*Center*), and 7 and 17 (*Right*) over a 96-h period.

did not reach significant levels (data not shown). We examined three combinations of chromosomes over a 96-h period. This period covered all peaks of TA formation (Fig. 4*B*). As shown in Fig. 7, we observed a change in overlaps between chromosomes 5 (red) and 13 (green) over the time course (Figs. 7 *A* and *B*). Both chromosomes were found in closer vicinity as the cells entered into the first TA cycle. Chromosomes 10 (green) and 7 (red) also showed increases in the percentage of overlap (Fig. 7 *A* and *B*), as did chromosomes 7 (red) and 17 (green) (Fig. 7 *A* and *B*). Representative 3D movies are shown in Movies 1–3.

## Discussion

**c-Myc Induces Telomeric Aggregates, Fusions, and BBF Cycles.** Previous studies have shown that c-Myc triggers a complex network of genomic instability at the level of single genes (14, 15, 19) and whole chromosomes (16–18) (for review, see ref. 13). In addition, c-Myc induces illegitimate replication initiation (19, 20), chromosomal rearrangements (18), DNA breakage, alterations of DNA repair (21–23), and a low level of point mutations (24, 25). A previously uncharacterized mechanism underlying c-Myc-dependent genomic instability at the chromosomal level directly affects the integrity of the telomeres and was revealed in this study.

The clear periodicity of the TA cycles that was found with four different Myc-activating treatments suggested a biological relevant Myc-dependent process. Theoretically, cycles of Myc-induced TAs could reflect (*i*) nuclear remodeling with the transient association and subsequent dissociation of telomeres; (*ii*) end-to-end chromosomal fusions that initiate BBF cycles (52, 53); (*iii*) c-Myc induced cell death; and (*iv*) a combination of all of the above. Our data are consistent with BBF cycles and exclude apoptosis as a direct contributor to the TA cycles. Apoptosis occurred at equal levels throughout the study and consistently reached about twice the levels seen in the control cells. The loss of cells was compensated by a 2-fold increase in proliferation in MycER-activated PreB (19). These data also indicate that there is genetic separation of genomic instability and apoptosis as reported in ref. 54. Whether telomere associations and dissociations (55) contributed to the TA cycles is presently unknown.

Direct evidence of BBF cycles in the periodicity of TAs came from a detailed analysis of chromosomal fusions, breakage, and rearrangements observed over the time course of five TA cycles. We demonstrated the occurrence of end-to-end fusions that generated dicentric chromosomes and breaks during anaphase, leaving one chromosome or chromatid with a piece from another chromosome or chromatid. The resulting telomere-free ends continue to undergo fusions with other chromosomes, a cycle of events termed BBF cycle (52, 53). Experimental data support these events from fusions to breakages and nonreciprocal translocations. The periodicity of the TA cycles is consistent with a ~12 h population doubling time of the PreB cells (19). Each peak of TAs is consistent with the repeated formation of TAs. Time points after the peak are in agreement with the breakage of dicentric chromosomes. Telomere-free ends initiate new BBF cycle(s) until no more telomere-free chromosomal end(s) persist.

**From Telomeres to Chromosomal Rearrangements: A New Pathway of c-Myc-Dependent Genomic Instability.** Muller (52) and McClintock (53) first described BBF cycles, a mechanism of chromosomal end-to-end fusion that contributes to the onset of genomic instability. BBF cycles contribute to deletions, gene amplification, nonreciprocal translocation, and overall genetic changes that are associated with tumorigenesis (56–63).

Our study showed that c-Myc is one key factor that initiates genomic instability through BBF cycles. Such BBF cycles in telomerase-positive immortalized mouse PreB cells (unpublished data) with long telomeres are distinct from BBF cycles reported for critically short telomeres (61, 64). Some TAs (but not necessarily all) represent fusions, as evident by the analysis of metaphase chromosomes. TAs and end-to-end fusions depended on time and levels of c-Myc activation. Analysis of frequencies of both events showed that they are closely linked. As the fusions initiate BBF cycles, the frequencies of breakage and nonreciprocal translocations increase over time.

A previously uncharacterized pathway of c-Myc-dependent genomic instability thus starts at the telomeric ends of the chromosomes. Both TAs and BBF cycles are the manifestation of deregulated Myc expression, leading to chromosomal rearrangements and subsequently to genomic instability.

Local chromosome movement increases chromosomal overlap in the nucleus. This temporal change in local positioning may permit the direct contact of chromosomal ends and facilitate recombinations and/or fusions. Such movements were observed after c-Myc deregulation and suggested an impact of the oncoprotein on local nuclear positioning of chromosomes. Chromosome movements were previously studied and found by others as well (65–69).

Several regulatory pathways involving oncogene deregulation may affect the 3D nuclear organization. Oncoproteins, including c-Myc, can alter the 3D nuclear organization and the organization of chromatin (70–72). They also affect the nuclear matrix. High mobility group protein I(Y) (HMGI(Y)) is a c-Myc-dependent nuclear matrix protein (73) with increased expression during neoplasia (2). The analysis of *myc*-binding sites in the human genome suggests that c-Myc binds to genes encoding nucleoskeletal components (74). Furthermore, constitutive c-Myc expression was shown to be associated with down-regulation of the telomere repeat binding protein TRF2 (10), a protein required for telomere capping and genome stability (75). Myc is also involved in the regulation of DNA repair (22, 23) and has been shown to induce DNA breakage (21). Thus taken together, many different c-Myc-dependent mechanisms could potentially affect the nuclear organization and, as shown here, converge at the telomeres.

We thank Dr. Michael Mowat for critical reading of this manuscript, Mary Cheang for statistical analyses, and Cheryl Taylor-Kashton and Landon Wark for deconvolution. The work was supported by the Canada Foundation for Innovation, the Canadian Institutes of Health Research, CancerCare Manitoba (S.M.), Fondation de France (Paris) and French Minister of Foreign Affairs (T.F.), Sander-Stiftung, and Deutsche Krebshilfe (P.B.), the Physics for Technology program of the Foundation for Fundamental Research in Matter, the Delft Inter-Faculty Research Center Life Tech, Cytiron, and the Delft Research program Life Science and Technology (Delft, The Netherlands).

1. Pierce, K. J., Pierce, A. W. & Crelley, D. S. (1989) *Cancer Res.* **49**, 2525–2532.
2. Lemon, E. S., Mulligan, M. C., Brumagel, G., Takalau, N., *Colley*, D. S. & Gelfenberg, R. H. (2002) *J. Cell Biochem.* **88**, 599–608.
3. Zink, D., Fischer, A. H. & Nickerson, J. A. (2004) *Nat. Rev. Cancer* **4**, 677–687.
4. Parada, L. A., McQueen, P. G., Munson, P. J. & Misteli, T. (2002) *Curr. Biol.* **12**, 1692–1697.
5. Parada, L. & Misteli, T. (2002) *Trends Cell Biol.* **12**, 425–432.
6. Rowe, J. T., McQueen, P. G., Munson, P. J., Parada, L. A. & Misteli, T. (2003) *Nat. Genet.* **34**, 287–291.
7. Parada, L. A., McQueen, P. G. & Misteli, T. (2004) *Genome Biol.* **5**, R44.
8. Neves, H., Ramos, C., da Silva, M. G., Parreira, A. & Parreira, L. (1999) *Blood* **93**, 1197–1207.
9. Cheung, T. C., Mushin, S., Granni, Y., Cheung, A. Y., Yeung, J. T., Vermeulen, B., van den Doel, R., Mongey, V., Petrin, M., Bratin, M., *et al.* (2004) *BMC Biol.* **2**, 12.
10. Ermler, S., Krunic, D., Knoch, T. A., Moshir, S., Mai, S., Greulich-Bode, K. M. & Boukamp, P. (2004) *Eur. J. Cell Biol.* **83**, 681–690.
11. Nesbit, C. E., Tersak, J. M. & Prochownik, E. V. (1999) *Oncogene* **18**, 3004–3016.
12. Potter, M. & Mattes, K. B. (1997) *Curr. Top. Microbiol. Immunol.* **224**, 1–17.
13. Mai, S. & Mushinski, J. F. (2003) *J. Environ. Pathol. Toxicol. Oncol.* **22**, 179–198.
14. Mai, S. (1994) *Gene* **148**, 253–260.
15. Mai, S., Hanley-Hyde, J. & Flint, M. (1996) *Oncogene* **12**, 277–288.
16. Mai, S., Flint, M., Stewart, D. & Happi, K. (1998) *Chromosome Res.* **4**, 365–371.
17. Felsher, D. W. & Bishop, J. M. (1999) *Proc. Natl. Acad. Sci. USA* **96**, 3940–3944.
18. Rockwood, L. D., Torrey, T. A., Kim, J. S., Coleman, A. E., Kowalchik, A. L., Xiang, S., Rice, T., Morse, H. C., 3rd, & Janz, S. (2002) *Oncogene* **21**, 7235–7248.
19. Kuschak, T. I., Kuschak, B. C., Taylor, C. L., Wright, J. A., Wiener, F. & Mai, S. (2002) *Oncogene* **21**, 909–920.
20. Louis, S. F., Grabher, B. & Mai, S. (2005) *Prog. Oncog.*, in press.
21. Vafa, O., Wade, M., Kern, S., Beeche, M., Pandita, T. K., Hampton, G. M. & Wahl, G. M. (2002) *Mol. Cell* **9**, 1031–1044.
22. Hiramoto, K., Factor, V. M., Calvisi, D. F., Conner, E. A. & Thorgeirsson, S. S. (2003) *Lab. Invest.* **83**, 643–654.
23. Karlsson, A., Deb-Basu, D., Cherry, A., Turner, S., Ford, J. & Felsher, D. W. (2003) *Proc. Natl. Acad. Sci. USA* **100**, 9974–9979.
24. Pattle, M. M., Hosier, E., Robinson, H., McCormick, C. J., Crouch, D. H., Durant, S. T., Matheson, E. C., Hall, A. G., Gillespie, D. A. & Brown, R. (2003) *Oncogene* **22**, 819–825.
25. Chiang, Y. C., Teng, S. C., Su, Y. N., Hsieh, F. J. & Wu, K. J. (2003) *J. Biol. Chem.* **278**, 19286–19291.
26. Adams, J. M., Harris, A. W., Pinkert, C. A., Corcoran, L. M., Alexander, W. S., Cory, S., Palmiter, R. D. & Brinster, R. L. (1985) *Nature* **318**, 533–538.
27. Potter, M. & Wiener, F. (1992) *Carcinogenesis* **13**, 1681–1697.
28. Pelengaris, S., Khan, M. & Evan, G. I. (2002) *Cell* **109**, 321–334.
29. Felsher, D. W. & Bishop, J. M. (1999) *Mol. Cell* **4**, 199–207.
30. Marinkovic, D., Marinkovic, T., Mahr, B., Hess, J. & Wirth, T. (2004) *Int. J. Cancer* **110**, 329–342.
31. D'Cruz, C. M., Gunther, E. J., Boxer, R. B., Hartman, J. L., Sintasath, L., Moody, S. E., Cox, J. D., Ha, S. I., Belka, G. K., Golant, A., Cardiff, R. D. & Chodosh, L. A. (2001) *Nat. Med.* **7**, 235–239.
32. Jun, M., Arvanitis, C., Cleti, K., Dewey, W., Leonhardt, E., Trinh, M., Sundberg, C. D., Bishop, J. M. & Felsher, D. W. (2002) *Science* **297**, 102–104.
33. Karlsson, A., Giannini, S., Tang, F., Fung-Weier, J., Tavan, G. & Felsher, D. W. (2003) *Blood* **101**, 2797–2803.
34. Strachan, C. M., Kogelman, A. M., Arvanitis, C., Karlsson, A., Beer, S., Mandl, S., Bachmann, M. H., Borowsky, A. D., Ruebner, B., Cardiff, R. D., *et al.* (2004) *Nature* **431**, 1112–1117.
35. Post, T., Mongey, V., Dalstein, V., Hagarcy, M., Mollette, D., Silva, S. & Mai, S. (2002) *Oncogene* **21**, 2981–2990.
36. Mai, S., Hanley-Hyde, J., Rainey, G. J., Kuschak, T. I., Paul, J. T., Littlewood, T. D., Mushak, H., Stevens, L. M., Henderson, D. W. & Mushinski, J. F. (1999) *Neoplasia* **1**, 241–252.
37. Wiener, F., Kuschak, T. I., Obata, S. & Mai, S. (1999) *Proc. Natl. Acad. Sci. USA* **96**, 13967–13972.
38. Wiener, F., Coleman, A., Mock, B. A. & Potter, M. (1995) *Cancer Res.* **55**, 1181–1188.
39. Littlewood, T. D., Hancock, D. C., Danielian, P. S., Parker, M. G. & Evan, G. I. (1995) *Nucleic Acids Res.* **23**, 1686–1690.
40. Greenman, S., Shapira, A. & Carey, T. E. (1986) *Gynecol. Oncol.* **30**, 228–238.
41. Greenman, S. E., Roberts, J. A., England, B. G., Granrose, M. & Carey, T. E. (1988) *Gynecol. Oncol.* **30**, 239–250.
42. Mandliker, S., Hebbar, V., Chrisos, K. & Kung, A. N. (2000) *Cancer Res.* **60**, 6691–6696.
43. Fukazawa, K., Wiener, F., Vande Woude, G. F. & Mai, S. (1997) *Oncogene* **15**, 1295–1302.
44. Figueroa, B., Lindermaier, H., Hergenhahn, M., Nieken, K. V. & Boukamp, P. (2000) *Cancer Res.* **60**, 2770–2774.
45. Schaefer, L. H., Schuster, D. & Herz, H. (2001) *J. Microsc.* **204**, 99–107.
46. Vermeulen, B. J., Gatini, Y., Mai, S., Mongey, V., Fest, T., Cheung, T. C. Y., Cheung, A. Y. C., Wark, L. & Young, I. T. (2005) *Cytometry*, in press.
47. Poon, S. S., Martens, U. M., Ward, R. K. & Lansdorp, P. M. (1999) *Cytometry* **36**, 267–278.
48. Beatty, B., Mai, S. & Squire, J., eds. (2002) *FISH: A Practical Approach* (Oxford Univ. Press, Oxford).
49. Benedetti, K., Chitsaba, T., Klein, G., Wiener, F. & Mai, S. (2004) *Chromosome Res.* **12**, 777–785.
50. Smith, G., Taylor-Kashton, C., Dashnicky, L., Symons, S., Wright, J. & Mai, S. (2003) *Neoplasia (Boston)* **5**, 110–120.
51. Wilson, E. B. (1927) *J. Am. Stat. Assoc.* **22**, 209–212.
52. Mueller, H. J. (1938) *Collecting Net.* **13**, 181–198.
53. McClintock, B. (1961) *Genetics* **26**, 234–282.
54. Fest, T., Gattei, A., Williams, G., Silva, S. & Mai, S. (2005) *Oncogene* **24**, 2944–2955.
55. Molenaar, C., Wiesmeijer, K., Verwoerd, N. P., Khazen, S., Eils, R., Tanke, H. J. & Dirks, R. W. (2003) *EMBO J.* **22**, 6631–6641.
56. DePinho, R. A. & Polyak, K. (2004) *Nat. Genet.* **36**, 932–934.
57. Arcandi, S. E., Chang, S., Lee, S. L., Alson, S., Gottlieb, G. J., Chin, L. & DePinho, R. A. (2000) *Nature* **406**, 641–645.
58. Arcandi, S. E. (2002) *Trends Mol. Med.* **8**, 44–47.
59. Smith, K. A., Stark, M. B., Gorman, P. A. & Stark, G. R. (1992) *Proc. Natl. Acad. Sci. USA* **89**, 5427–5431.
60. Cailly, M., Debily, M. A., Rosier, L., Autiero, M., Billault, A., Mayau, V., El Marhomy, S., Guardiola, J., Bernheim, A., Couillin, P., *et al.* (2002) *Hum. Mol. Genet.* **11**, 2887–2899.
61. Hande, M. P., Samper, E., Lansdorp, P. & Blasco, M. A. (1999) *J. Cell Biol.* **144**, 589–601.
62. Murnane, J. P. & Sabatier, L. (2004) *Bioessays* **26**, 1164–1174.
63. Gisselsson, D., Jonson, T., Petersen, A., Strombeck, B., Dal Cin, P., Hoglund, M., Mitelman, F., Mertens, F. & Mandahl, N. (2001) *Proc. Natl. Acad. Sci. USA* **98**, 12683–12688.
64. Londono-Vallejo, J. A. (2004) *Cancer Lett.* **212**, 135–144.
65. Zink, D. & Cremer, T. (1998) *Curr. Biol.* **8**, R321–R324.
66. Walter, J., Schermelleh, L., Cremer, M., Tashiro, S. & Cremer, T. (2003) *J. Cell Biol.* **160**, 685–697.
67. Visser, A. E., Taslerin, D., Boyle, A. L. & Ward, D. C. (1998) *Exp. Cell Res.* **205**, 142–151.
68. Ferguson, M. & Ward, D. C. (1992) *Chromosoma* **101**, 557–565.
69. Bridger, J. M., Boyle, S., Kill, I. R. & Bickmore, W. A. (2000) *Curr. Biol.* **10**, 149–152.
70. Fischer, A. H., Bond, J. A., Taylenson, P., Battler, D. E. & Wynford-Thomas, D. (1998) *Am. J. Pathol.* **153**, 1443–1450.
71. Fischer, A. H., Chadee, D. N., Wright, J. A., Gamder, T. S. & Davie, J. R. (1998) *J. Cell Biochem.* **70**, 130–140.
72. Chadee, D. N., Hendzel, M. J., Tylpinki, C. P., Allis, C. D., Bazett-Jones, D. P., Wright, J. A. & Davie, J. R. (1999) *J. Biol. Chem.* **274**, 24914–24920.
73. Tokuhu, N., Hawkins, A. L., Griffin, C. A., Isaacs, W. B. & Coffey, D. S. (2002) *Cancer Res.* **62**, 643–651.
74. Fernandez, P. C., Frank, S. R., Wang, L., Schroeder, M., Liu, S., Greene, J., Cocito, A. & Amati, B. (2003) *Genes Dev.* **17**, 1115–1129.
75. van Steensel, B., Smogorzewska, A. & de Lange, T. (1998) *Cell* **92**, 401–413.

# III. DISCUSSION

## 3.1 Telomere and Its 3D Nuclear Organization in Normal and Tumor Cells

Recent advancements in molecular imaging allow us to study the temporal and spatial organization of telomeres in the interphase nucleus of mammalian cells in 3D space. Weierich et al., 2003 and Chuang et al., 2004 have shown that telomeres are organized in a dynamic cell cycle- and tissue-dependent manner in normal cells (Chuang et al., 2004; Weierich et al., 2003). The 3D telomere distribution in the nucleus can be determined by the ratio of two different nuclei, or a/c ratio (Chuang et al., 2004; Vermolen et al., 2005). When the cells are in G0/G1 and S phases of the cell cycle, the telomeres distribute throughout the entire nuclear space and give a small a/c ratio. When the cell is in G2 phase, telomeres align in the center of the nucleus and form a telomeric disk (Chuang et al., 2004) and give a large a/c ratio due to the disk-like organization of telomeres. Chuang et al. described this by using the primary mouse lymphocyte as an example. The a/c ratios for telomeric position in G0/G1, S, and G2 are 1.4±0.1, 1.5±0.2, and 14±2 respectively. Dynamic telomere organization has been visualized by live cell imaging of human osteosarcoma (U2OS), human cervical carcinoma (HeLa), and mouse MS5 cells. Both short and long ranges of movements were observed over a period of 20 minutes (Molenaar et al., 2003). In addition to cell cycle dependency, dynamic telomere movement also depends on the shape of the nucleus (Chuang et al.,

2004; Ermler et al., 2004). *In vivo* mobility studies by Bronstein et al. have shown that telomere dynamics govern the short-term anomalous diffusion while telomere binding governs the long-term diffusion which altogether contribute to 3D telomeric organization in the nucleus. Therefore we conclude that telomere organization within the nucleus is dynamic, moving in cell cycle- and cell type-dependent manner (Bronstein et al., 2009; Chuang et al., 2004).

Recent work presented by De Vos et al. confirmed our findings of telomere organization (De Vos et al., 2009). Microterritories occupied by several telomeric ends are visualized using the controlled light exposure microscopy (CLEM). Such close proximity of telomere neighborhood organization can facilitate recombination at the subtelomeric regions which can lead to genomic instability. Additional work can be done in the future with high-resolution microscopy methods to better delineate the chromosomal ends.

There are two major phenotypes of telomeric dysfunction in tumor cells. The first phenotype is critically short telomeres (DePinho and Polyak, 2004). The second phenotype is formation of telomeric aggregates (TAs) independent of telomere size or telomerase activity (Chuang et al., 2004; Louis et al., 2005). It was shown that each telomere of a normal cell occupies its specific 3D space within the nucleus without overlapping or forming aggregates with other telomeres (Chuang et al., 2004). In contrast, different sizes and numbers of TAs are observed in tumor cells (Chuang et al., 2004; Louis et al., 2005). Both phenotypes can lead to breakage-bridge-fusion (BBF) that contribute to genomic

instability (Artandi et al., 2000; DePinho and Polyak, 2004; Murnane and Sabatier, 2004).

### 3.2 Telomere Remodeling and Chromosomal Aberrations in the 3D Interphase Nucleus

Dynamic alterations of 3D nuclear structures can potentiate genomic instability. When telomeres form aggregates in the 3D nucleus of tumor cells, some of them fuse together and form dicentric chromosomes. When these end-to-end fused chromosomes divide, they form the anaphase bridge first and then break apart, leaving one chromosome with a terminal deletion and another one with a translocated piece. Both chromosomes have telomere free ends, which represent double-stranded DNA break, can fuse with other chromosomes. This BBF cycle was first described by Muller and McClintock (McClintock, 1941; McClintock, 1942; Müller, 1938). Louis et al. showed conditional c-Myc deregulation can induce cycles of telomeric aggregates in interphase nuclei. The resulting BBF cycles lead to chromosomal rearrangements and the onset of genomic instability (Louis et al., 2005). .

### 3.3 Mechanism of Altered Telomeric Nuclear Organization

In the study by Louis et al conditionally de-regulated c-*Myc* oncogene leads to generation of cycles of TAs over 144 hours that was past the initial c-*Myc* deregulation (Louis et al., 2005). This suggests that the oncoprotein is no longer required for the downstream effects of subsequent cycles of TA formation.

The time of c-*Myc* deregulation was proportional to the number of TA cycles observed. As a result of c-*Myc* deregulation, TA formation precedes chromosomal end-to-end fusions and the onset of chromosomal instability. Fusion of telomeric ends can be confirmed by the presence of inter-nuclear bridge and dicentric chromosomes as cells progress through the cell cycle.

c-*Myc*-induced TA formation is independent of critical shortening of telomeric end and telomerase activity. However, formation of TA has been observed in critically shortened telomeres in Hodgkin lymphoma cells (Knecht et al., 2010).

It has been shown that Myc box II mutant is unable to induce TA formation (Caporali et al., 2007). This indicates the Myc box II is a conserved element within the N-terminus of c-*Myc* is needed for all known functions of c-Myc (Stone et al., 1987). Only full length c-*Myc* but not myc box II mutant *Myc* is able to induce tumor formation in SCID mice (Fest et al., 2005).

## 3.4 Applications of 3D Telomere and Chromosome Organization in Medicine

### 3.4.1 Mechanism of Disease

Formation of TAs have been described in various tumor cell lines and primary tumors, including human Burkitt lymphoma, neuroblastoma and colon carcinoma and primary mouse plasmacytoma and primary human head and neck squamous cell carcinoma and glioblastoma (Chuang et al., 2004; Gadji et al.,

2010; Mai and Garini, 2006), It is shown that the telomere dysfunction is involved in the transition of the Hodgkin cells (H cells) to the Reed-Sternberg cells (RS cells) (Knecht et al., 2009). In addition, significant telomere shortening and formation of TAs were observed in RS cells in EBV positive Hodgkin's lymphoma (Knecht et al., 2010). These telomere-poor or telomere-free "ghost" nuclei are formed in end-stage tumor cells which are incapable of dividing. Additional work to elucidate the structural organization of chromosomes in the RS cells will be of interest in understanding the nature of progression of Hodgkin's lymphoma.

### 3.4.2 Cancer Biomarkers

The topic of cancer biomarkers is broad and involves multiple disciplines of science and technology. The 3D positioning patterns of telomeres and chromosomes can be used as diagnostic and prognostic biomarkers in the near future. Specific 3D alterations in the relative arrangement of chromosome territories may be specific to a disease entity. As telomere dysfunction occurs prior to chromosomal re-arrangement (Louis et al., 2005), telomeric aggregates can be an attractive biomarker for early detection.

In the paper presented by Gadji et al, the 3D telomeric profile that was characteristic of each group correlated with short-term, intermediate and long-term survival and time to progression in a patient cohort of 11 individuals (Gadji et al., 2010). The three telomeric signatures including the total number of telomeres and the nuclear distribution and presence of TAs were evaluated using

the Teloview program and the SpotScan system. This study indicates a correlation between clinical outcome parameters and 3D telomere organization. In addition, the new SpotScan system provides a high throughput means to assess TAs. This may be important in time-critical situations such as assessing intra-operative frozen sections performed during oncologic surgery. The 3D nuclear structure thus can be of prognostic, predictive value and possibly provide pharmacodynamic biomarkers, to provide information on natural course of disease, treatment response and optimal dose of experimental therapeutic agents, respectively.

### 3.4.3 Molecular Marker in Other Disease Processes

The first observation of TAs in 3D space was made in tumor cells. However, additional studies have confirmed that TAs are present in other conditions and diseases in different tissue types and body fluids. Examples include the formation of TAs with various numbers and sizes during senescence of human mesenchymal stem cells (Raz et al., 2008) and were found in the placenta of pregnant women with pre-eclampsia (Sukenik-Halevy et al., 2009), amniocytes from pregnant women carrying trisomy 21 fetuses (Hadi et al., 2009) and leukocytes from chronic hepatitis C patients (Amiel et al., 2009). The potential mechanisms for TA formation in different diseases may include oxidative stress, inflammation and infection. Therefore we propose that TAs can be used as a new diagnostic and prognostic tool for different disease entities. TAs may represent a new class of biomarker, namely the optical biomarker.

Future studies to unravel the nature of disease and the process of the disease development and disease progression can be performed from a different perspective via observation of aberrant 3D organization of telomere and chromosomal organizations. The latter will in turn allow us to understand “cancer as a disease of DNA organization and cell structure” (Pienta et al., 1989) and other disease processes in humans.

## IV. References

Abbe, E. (1873). Beiträge zur Theorie des Mikroskopes und der mikroskopischen Wahrnehmung. Arch Mikroskop Anat, 413–468.

Agard, D. A., and Sedat, J. W. (1983). Three-dimensional architecture of a polytene nucleus. Nature *302*, 676-681.

Airy, G. B. (1835). On the diffraction of an object-glass with circular apeture. Trans Cambridge Phil Soc *5*, 283-291.

Akhtar, A., and Gasser, S. M. (2007). The nuclear envelope and transcriptional control. Nat Rev Genet *8*, 507-517.

Amiel, A., Fejgin, M. D., Goldberg-Bittman, L., Sharoni, R., Hadary, R., and Kitay-Cohen, Y. (2009). Telomere aggregates in hepatitis C patients. Cancer Invest *27*, 650-654.

Anselmo, N. P., Rey, J. A., Almeida, L. O., Custodio, A. C., Almeida, J. R., Clara, C. A., Santos, M. J., and Casartelli, C. (2009). Concurrent sequence variation of TP53 and TP73 genes in anaplastic astrocytoma. Genet Mol Res *8*, 1257-1263.

Artandi, S. E., Chang, S., Lee, S. L., Alson, S., Gottlieb, G. J., Chin, L., and DePinho, R. A. (2000). Telomere dysfunction promotes non-reciprocal translocations and epithelial cancers in mice. Nature *406*, 641-645.

Baek, J. Y., Morris, S. M., Campbell, J., Fausto, N., Yeh, M. M., and Grady, W. M. (2009). TGF-ss inactivation and TGF-alpha overexpression cooperate in an in vivo mouse model to induce hepatocellular carcinoma that recapitulates molecular features of human liver cancer. Int J Cancer.

Balkwill, F., Charles, K. A., and Mantovani, A. (2005). Smoldering and polarized inflammation in the initiation and promotion of malignant disease. Cancer Cell *7*, 211-217.

Balkwill, F., and Mantovani, A. (2001). Inflammation and cancer: back to Virchow? Lancet *357*, 539-545.

Beckman, R. A., and Loeb, L. A. (2005). Genetic instability in cancer: theory and experiment. Semin Cancer Biol *15*, 423-435.

Berezney, R. (2002). Regulating the mammalian genome: the role of nuclear architecture. Adv Enzyme Regul *42*, 39-52.

Bhatia, K., Huppi, K., Spangler, G., Siwarski, D., Iyer, R., and Magrath, I. (1993). Point mutations in the c-Myc transactivation domain are common in Burkitt's lymphoma and mouse plasmacytomas. Nat Genet *5*, 56-61.

Blackburn, E. H. (2001). Switching and signaling at the telomere. Cell *106*, 661-673.

Blasco, M. A. (2007). The epigenetic regulation of mammalian telomeres. Nat Rev Genet *8*, 299-309.

Boveri, T. (1902). Uber mehrpolige Mitosen als Mittel zur Analyse des Zellkerns. Verh Phys Med Gesellschaft Wurzburg *35*, 67-90.

Boyle, W. S., and Smith, G. E. (1970). Bell Systems Technical Journal, 587.

Bradley, K. T., Budnick, S. D., and Logani, S. (2006). Immunohistochemical detection of p16INK4a in dysplastic lesions of the oral cavity. Mod Pathol *19*, 1310-1316.

Bronstein, I., Israel, Y., Kepten, E., Mai, S., Shav-Tal, Y., Barkai, E., and Garini, Y. (2009). Transient anomalous diffusion of telomeres in the nucleus of mammalian cells. Phys Rev Lett *103*, 018102.
Bryan, T. M., Englezou, A., Gupta, J., Bacchetti, S., and Reddel, R. R. (1995). Telomere elongation in immortal human cells without detectable telomerase activity. Embo J *14*, 4240-4248.
Califano, J., Ahrendt, S. A., Meininger, G., Westra, W. H., Koch, W. M., and Sidransky, D. (1996). Detection of telomerase activity in oral rinses from head and neck squamous cell carcinoma patients. Cancer Res *56*, 5720-5722.
Campisi, J. (2000). Cancer, aging and cellular senescence. In Vivo *14*, 183-188.
Caporali, A., Wark, L., Vermolen, B. J., Garini, Y., and Mai, S. (2007). Telomeric aggregates and end-to-end chromosomal fusions require myc box II. Oncogene *26*, 1398-1406.
Casella, M. L., Fanni, V. S., Verndl, D. O., Basso, M. C., Mello, L. F., and Glina, S. (2009). Schistosomiasis mansoni of the bladder simulating bladder cancer: a case report. Rev Soc Bras Med Trop *42*, 581-582.
Choi, Y. H., Ahn, J. H., Kim, S. B., Jung, K. H., Gong, G. Y., Kim, M. J., Son, B. H., Ahn, S. H., and Kim, W. K. (2009). Tissue microarray-based study of patients with lymph node-negative breast cancer shows that HER2/neu overexpression is an important predictive marker of poor prognosis. Ann Oncol *20*, 1337-1343.
Chuang, T. C., Moshir, S., Garini, Y., Chuang, A. Y., Young, I. T., Vermolen, B., van den Doel, R., Mougey, V., Perrin, M., Braun, M.*, et al.* (2004). The three-dimensional organization of telomeres in the nucleus of mammalian cells. BMC Biol *2*, 12.
Connor, J. A. (1986). Digital imaging of free calcium changes and of spatial gradients in growing processes in single, mammalian central nervous system cells. Proc Natl Acad Sci U S A *83*, 6179-6183.
Costa, A., Daidone, M. G., Daprai, L., Villa, R., Cantu, S., Pilotti, S., Mariani, L., Gronchi, A., Henson, J. D., Reddel, R. R., and Zaffaroni, N. (2006). Telomere maintenance mechanisms in liposarcomas: association with histologic subtypes and disease progression. Cancer Res *66*, 8918-8924.
Coussens, L. M., and Werb, Z. (2002). Inflammation and cancer. Nature *420*, 860-867.
Cremer, M., Kupper, K., Wagler, B., Wizelman, L., von Hase, J., Weiland, Y., Kreja, L., Diebold, J., Speicher, M. R., and Cremer, T. (2003). Inheritance of gene density-related higher order chromatin arrangements in normal and tumor cell nuclei. J Cell Biol *162*, 809-820.
Cremer, T., and Cremer, C. (2001). Chromosome territories, nuclear architecture and gene regulation in mammalian cells. Nat Rev Genet *2*, 292-301.
Cremer, T., Cremer, M., Dietzel, S., Muller, S., Solovei, I., and Fakan, S. (2006). Chromosome territories--a functional nuclear landscape. Curr Opin Cell Biol *18*, 307-316.
de Lange, T. (2002). Protection of mammalian telomeres. Oncogene *21*, 532-540.

de Lange, T. (2005). Shelterin: the protein complex that shapes and safeguards human telomeres. Genes Dev *19*, 2100-2110.
De Vos, W. H., Hoebe, R. A., Joss, G. H., Haffmans, W., Baatout, S., Van Oostveldt, P., and Manders, E. M. (2009). Controlled light exposure microscopy reveals dynamic telomere microterritories throughout the cell cycle. Cytometry A *75*, 428-439.
Dechat, T., Pfleghaar, K., Sengupta, K., Shimi, T., Shumaker, D. K., Solimando, L., and Goldman, R. D. (2008). Nuclear lamins: major factors in the structural organization and function of the nucleus and chromatin. Genes Dev *22*, 832-853.
Del Casar, J. M., Carreno, G., Gonzalez, L. O., Junquera, S., Gonzalez-Reyes, S., Gonzalez, J. M., Bongera, M., Merino, A. M., and Vizoso, F. J. (2009). Expression of metalloproteases and their inhibitors in primary tumors and in local recurrences after mastectomy for breast cancer. J Cancer Res Clin Oncol.
DePinho, R. A., and Polyak, K. (2004). Cancer chromosomes in crisis. Nat Genet *36*, 932-934.
Dundr, M., and Misteli, T. (2001). Functional architecture in the cell nucleus. Biochem J *356*, 297-310.
Dunham, M. A., Neumann, A. A., Fasching, C. L., and Reddel, R. R. (2000). Telomere maintenance by recombination in human cells. Nat Genet *26*, 447-450.
Ellinger, P. H., and Hirt, A. (1929). Mikroskopische Beobachtungen an lebenden Organen mit Demonstrationen (Intravitalmikroskopie). Arch Exp Pathol Phar 63.
Ermler, S., Krunic, D., Knoch, T. A., Moshir, S., Mai, S., Greulich-Bode, K. M., and Boukamp, P. (2004). Cell cycle-dependent 3D distribution of telomeres and telomere repeat-binding factor 2 (TRF2) in HaCaT and HaCaT-myc cells. Eur J Cell Biol *83*, 681-690.
Erwin, J. A., and Lee, J. T. (2008). New twists in X-chromosome inactivation. Curr Opin Cell Biol *20*, 349-355.
Fest, T., Guffei, A., Williams, G., Silva, S., and Mai, S. (2005). Uncoupling of genomic instability and tumorigenesis in a mouse model of Burkitt's lymphoma expressing a conditional box II-deleted Myc protein. Oncogene *24*, 2944-2953.
Fidler, I. J. (2003). The pathogenesis of cancer metastasis: the 'seed and soil' hypothesis revisited. Nat Rev Cancer *3*, 453-458.
Foulds, L. (1957). Tumor progression. Cancer Res *17*, 355-356.
Fraser, P., and Bickmore, W. (2007). Nuclear organization of the genome and the potential for gene regulation. Nature *447*, 413-417.
Freund, H. (1969). [The role of Max Haitinger in the development of fluorescence microscopy]. Mikroskopie *25*, 73-77.
Gadji, M., Fortin, D., Tsanaclis, A. M., Garini, Y., Katzir, N., Wienburg, Y., Yan, J., Klewes, L., Klonisch, T., Drouin, R., and Mai, S. (2010). Three-dimensional nuclear telomere architecture is associated with differential time to progression and overall survival in glioblastoma patients. Neoplasia *12*, 183-191.
Germani, R. M., Civantos, F. J., Elgart, G., Roberts, B., and Franzmann, E. J. (2009). Molecular markers of micrometastasis in oral cavity carcinomas. Otolaryngol Head Neck Surg *141*, 52-58.

Gibault, L., Metges, J. P., Conan-Charlet, V., Lozac'h, P., Robaszkiewicz, M., Bessaguet, C., Lagarde, N., and Volant, A. (2005). Diffuse EGFR staining is associated with reduced overall survival in locally advanced oesophageal squamous cell cancer. Br J Cancer *93*, 107-115.
Gilbert, D. M. (2001). Nuclear position leaves its mark on replication timing. J Cell Biol *152*, F11-15.
Gillison, M. L., Koch, W. M., Capone, R. B., Spafford, M., Westra, W. H., Wu, L., Zahurak, M. L., Daniel, R. W., Viglione, M., Symer, D. E.*, et al.* (2000). Evidence for a causal association between human papillomavirus and a subset of head and neck cancers. J Natl Cancer Inst *92*, 709-720.
Goldman, R. D., Gruenbaum, Y., Moir, R. D., Shumaker, D. K., and Spann, T. P. (2002). Nuclear lamins: building blocks of nuclear architecture. Genes Dev *16*, 533-547.
Gonzalez-Suarez, I., Redwood, A. B., Perkins, S. M., Vermolen, B., Lichtensztejin, D., Grotsky, D. A., Morgado-Palacin, L., Gapud, E. J., Sleckman, B. P., Sullivan, T.*, et al.* (2009). Novel roles for A-type lamins in telomere biology and the DNA damage response pathway. Embo J *28*, 2414-2427.
Green, D. R., and Kroemer, G. (2009). Cytoplasmic functions of the tumour suppressor p53. Nature *458*, 1127-1130.
Gruenbaum, Y., Margalit, A., Goldman, R. D., Shumaker, D. K., and Wilson, K. L. (2005). The nuclear lamina comes of age. Nat Rev Mol Cell Biol *6*, 21-31.
Guffei, A., Lichtensztejn, Z., Goncalves Dos Santos Silva, A., Louis, S. F., Caporali, A., and Mai, S. (2007). c-Myc-dependent formation of Robertsonian translocation chromosomes in mouse cells. Neoplasia *9*, 578-588.
Guijon, F. B., Greulich-Bode, K., Paraskevas, M., Baker, P., and Mai, S. (2007). Premalignant cervical lesions are characterized by dihydrofolate reductase gene amplification and c-Myc overexpression: possible biomarkers. J Low Genit Tract Dis *11*, 265-272.
Gullo, C., Low, W. K., and Teoh, G. (2008). Association of Epstein-Barr virus with nasopharyngeal carcinoma and current status of development of cancer-derived cell lines. Ann Acad Med Singapore *37*, 769-777.
Guney, K., Ozbilim, G., Derin, A. T., and Cetin, S. (2007). Expression of PTEN protein in patients with laryngeal squamous cell carcinoma. Auris Nasus Larynx *34*, 481-486.
Gupta, G. P., and Massague, J. (2006). Cancer metastasis: building a framework. Cell *127*, 679-695.
Hadi, E., Sharony, R., Goldberg-Bittman, L., Biron-Shental, T., Fejgin, M., and Amiel, A. (2009). Telomere aggregates in trisomy 21 amniocytes. Cancer Genet Cytogenet *195*, 23-26.
Hadzisejdic, I., Mustac, E., Jonjic, N., Petkovic, M., and Grahovac, B. (2010). Nuclear EGFR in ductal invasive breast cancer: correlation with cyclin-D1 and prognosis. Mod Pathol *23*, 392-403.
Haller, F., Lobke, C., Ruschhaupt, M., Cameron, S., Schulten, H. J., Schwager, S., von Heydebreck, A., Gunawan, B., Langer, C., Ramadori, G.*, et al.* (2008). Loss of 9p leads to p16INK4A down-regulation and enables RB/E2F1-dependent

cell cycle promotion in gastrointestinal stromal tumours (GISTs). J Pathol *215*, 253-262.
Hanahan, D., and Weinberg, R. A. (2000). The hallmarks of cancer. Cell *100*, 57-70.
Hansemann, D. (1890). Ueber asymmetrische Zelltheilung in Epithelkrebsen und deren biologische Bedeutung. [On the asymmetrical cell division in epithelial cancers and its biological significance]. Arch Pathol Anat etc Berl (Virchow's Arch) *119*, 299-326.
Hansemann, D. (1891). Ueber pathologishe mitosen. [On pathological mitoses]. Arch Pathol Anat etc Berl (Virchow's Arch) *123*, 356-370.
Hansemann, D. (1893). Studien uber die Spezificitat, den Altruismus und die Anaplasie der Zellen mit besonderer Berucksichtigung der Geschwulste. [Studies of the specificity, altruism and anaplasia of cells with special reference to tumours]. Berlin: A Hirschwald.
Harley, C. B., Futcher, A. B., and Greider, C. W. (1990). Telomeres shorten during ageing of human fibroblasts. Nature *345*, 458-460.
Harley, C. B., Vaziri, H., Counter, C. M., and Allsopp, R. C. (1992). The telomere hypothesis of cellular aging. Exp Gerontol *27*, 375-382.
Hayflick, L. (1965). The Limited in Vitro Lifetime of Human Diploid Cell Strains. Exp Cell Res *37*, 614-636.
Heimstädt, O. (1911). Das Fluoreszenzmikroskop. Z Wiss Mikrosk, 330–337.
Henson, J. D., Hannay, J. A., McCarthy, S. W., Royds, J. A., Yeager, T. R., Robinson, R. A., Wharton, S. B., Jellinek, D. A., Arbuckle, S. M., Yoo, J.*, et al.* (2005). A robust assay for alternative lengthening of telomeres in tumors shows the significance of alternative lengthening of telomeres in sarcomas and astrocytomas. Clin Cancer Res *11*, 217-225.
Hirsch, F. R., Varella-Garcia, M., and Cappuzzo, F. (2009). Predictive value of EGFR and HER2 overexpression in advanced non-small-cell lung cancer. Oncogene *28 Suppl 1*, S32-37.
Hooke, R. (1665). Micrographia: or Some Physiological Descriptions of Minute Bodies, Made by Magnifying Glasses with Observations and Inquiries Thereupon. James Allestry.
Hsu, H. P., Shan, Y. S., Jin, Y. T., Lai, M. D., and Lin, P. W. (2010). Loss of E-cadherin and beta-catenin is correlated with poor prognosis of ampullary neoplasms. J Surg Oncol.
Jeyapalan, J. N., Varley, H., Foxon, J. L., Pollock, R. E., Jeffreys, A. J., Henson, J. D., Reddel, R. R., and Royle, N. J. (2005). Activation of the ALT pathway for telomere maintenance can affect other sequences in the human genome. Hum Mol Genet *14*, 1785-1794.
Johnson, J. E., Varkonyi, R. J., Schwalm, J., Cragle, R., Klein-Szanto, A., Patchefsky, A., Cukierman, E., von Mehren, M., and Broccoli, D. (2005). Multiple mechanisms of telomere maintenance exist in liposarcomas. Clin Cancer Res *11*, 5347-5355.
Kammori, M., Kanauchi, H., Nakamura, K., Kawahara, M., Weber, T. K., Mafune, K., Kaminishi, M., and Takubo, K. (2002). Demonstration of human telomerase

reverse transcriptase in human colorectal carcinomas by in situ hybridization. Int J Oncol *20*, 15-21.
Kapatai, G., and Murray, P. (2007). Contribution of the Epstein Barr virus to the molecular pathogenesis of Hodgkin lymphoma. J Clin Pathol *60*, 1342-1349.
Karin, M., Lawrence, T., and Nizet, V. (2006). Innate immunity gone awry: linking microbial infections to chronic inflammation and cancer. Cell *124*, 823-835.
Kim, N. W., Piatyszek, M. A., Prowse, K. R., Harley, C. B., West, M. D., Ho, P. L., Coviello, G. M., Wright, W. E., Weinrich, S. L., and Shay, J. W. (1994). Specific association of human telomerase activity with immortal cells and cancer. Science *266*, 2011-2015.
Knecht, H., Sawan, B., Lichtensztejn, D., Lemieux, B., Wellinger, R. J., and Mai, S. (2009). The 3D nuclear organization of telomeres marks the transition from Hodgkin to Reed-Sternberg cells. Leukemia *23*, 565-573.
Knecht, H., Sawan, B., Lichtensztejn, Z., Lichtensztejn, D., and Mai, S. (2010). 3D Telomere FISH defines LMP1-expressing Reed-Sternberg cells as end-stage cells with telomere-poor 'ghost' nuclei and very short telomeres. Lab Invest.
Krepela, E., Dankova, P., Moravcikova, E., Krepelova, A., Prochazka, J., Cermak, J., Schutzner, J., Zatloukal, P., and Benkova, K. (2009). Increased expression of inhibitor of apoptosis proteins, survivin and XIAP, in non-small cell lung carcinoma. Int J Oncol *35*, 1449-1462.
Kress, C., Ballester, M., Devinoy, E., and Rijnkels, M. (2010). Epigenetic modifications in 3D: nuclear organization of the differentiating mammary epithelial cell. J Mammary Gland Biol Neoplasia *15*, 73-83.
Kumaran, R. I., Thakar, R., and Spector, D. L. (2008). Chromatin dynamics and gene positioning. Cell *132*, 929-934.
Kuschak, T. I., Kuschak, B. C., Taylor, C. L., Wright, J. A., Wiener, F., and Mai, S. (2002). c-Myc initiates illegitimate replication of the ribonucleotide reductase R2 gene. Oncogene *21*, 909-920.
Kuttler, F., and Mai, S. (2006). c-Myc, Genomic Instability and Disease. Genome Dyn *1*, 171-190.
Lamond, A. I., and Spector, D. L. (2003). Nuclear speckles: a model for nuclear organelles. Nat Rev Mol Cell Biol *4*, 605-612.
Lanctot, C., Cheutin, T., Cremer, M., Cavalli, G., and Cremer, T. (2007). Dynamic genome architecture in the nuclear space: regulation of gene expression in three dimensions. Nat Rev Genet *8*, 104-115.
Lansdorp, P. M. (2000). Repair of telomeric DNA prior to replicative senescence. Mech Ageing Dev *118*, 23-34.
Laud, P. R., Multani, A. S., Bailey, S. M., Wu, L., Ma, J., Kingsley, C., Lebel, M., Pathak, S., DePinho, R. A., and Chang, S. (2005). Elevated telomere-telomere recombination in WRN-deficient, telomere dysfunctional cells promotes escape from senescence and engagement of the ALT pathway. Genes Dev *19*, 2560-2570.
Le, S., Moore, J. K., Haber, J. E., and Greider, C. W. (1999). RAD50 and RAD51 define two pathways that collaborate to maintain telomeres in the absence of telomerase. Genetics *152*, 143-152.

Lee, J., and Hasteh, F. (2009). Oncocytic variant of papillary thyroid carcinoma associated with Hashimoto's thyroiditis: a case report and review of the literature. Diagn Cytopathol *37*, 600-606.
Lee, S. H., Lee, J. K., Jin, S. M., Lee, K. C., Sohn, J. H., Chae, S. W., and Kim, D. H. (2010). Expression of cell-cycle regulators (cyclin D1, cyclin E, p27kip1, p57kip2) in papillary thyroid carcinoma. Otolaryngol Head Neck Surg *142*, 332-337.
Lee, W. M., Schwab, M., Westaway, D., and Varmus, H. E. (1985). Augmented expression of normal c-myc is sufficient for cotransformation of rat embryo cells with a mutant ras gene. Mol Cell Biol *5*, 3345-3356.
Lengauer, C., Kinzler, K. W., and Vogelstein, B. (1998). Genetic instabilities in human cancers. Nature *396*, 643-649.
Li, X. H., Zheng, H. C., Takahashi, H., Masuda, S., Yang, X. H., and Takano, Y. (2009). PTEN expression and mutation in colorectal carcinomas. Oncol Rep *22*, 757-764.
Lichter, P., Cremer, T., Borden, J., Manuelidis, L., and Ward, D. C. (1988). Delineation of individual human chromosomes in metaphase and interphase cells by in situ suppression hybridization using recombinant DNA libraries. Hum Genet *80*, 224-234.
Lin, J., Guan, Z., Wang, C., Feng, L., Zheng, Y., Caicedo, E., Bearth, E., Peng, J. R., Gaffney, P., and Ondrey, F. G. Inhibitor of differentiation 1 contributes to head and neck squamous cell carcinoma survival via the NF-kappaB/survivin and phosphoinositide 3-kinase/Akt signaling pathways. Clin Cancer Res *16*, 77-87.
Lindsey, J., McGill, N. I., Lindsey, L. A., Green, D. K., and Cooke, H. J. (1991). In vivo loss of telomeric repeats with age in humans. Mutat Res *256*, 45-48.
Lindstrom, M. S., and Wiman, K. G. (2002). Role of genetic and epigenetic changes in Burkitt lymphoma. Semin Cancer Biol *12*, 381-387.
Liu, B., Ren, Z., Shi, Y., Guan, C., Pan, Z., and Zong, Z. (2008). Activation of signal transducers and activators of transcription 3 and overexpression of its target gene CyclinD1 in laryngeal carcinomas. Laryngoscope *118*, 1976-1980.
Liu, D., O'Connor, M. S., Qin, J., and Songyang, Z. (2004). Telosome, a mammalian telomere-associated complex formed by multiple telomeric proteins. J Biol Chem *279*, 51338-51342.
Loeb, L. A. (1991). Mutator phenotype may be required for multistage carcinogenesis. Cancer Res *51*, 3075-3079.
Longworth, M. S., and Dyson, N. J. (2010). pRb, a local chromatin organizer with global possibilities. Chromosoma *119*, 1-11.
Louis, S. F., Vermolen, B. J., Garini, Y., Young, I. T., Guffei, A., Lichtensztejn, Z., Kuttler, F., Chuang, T. C., Moshir, S., Mougey, V.*, et al.* (2005). c-Myc induces chromosomal rearrangements through telomere and chromosome remodeling in the interphase nucleus. Proc Natl Acad Sci U S A *102*, 9613-9618.
Lundblad, V., and Blackburn, E. H. (1993). An alternative pathway for yeast telomere maintenance rescues est1- senescence. Cell *73*, 347-360.

Machado, A. M., Figueiredo, C., Seruca, R., and Rasmussen, L. J. (2010). Helicobacter pylori infection generates genetic instability in gastric cells. Biochim Biophys Acta.
Mai, S., and Garini, Y. (2006). The significance of telomeric aggregates in the interphase nuclei of tumor cells. J Cell Biochem *97*, 904-915.
Mai, S., and Mushinski, J. F. (2003). c-Myc-induced genomic instability. J Environ Pathol Toxicol Oncol *22*, 179-199.
Mantovani, A., Allavena, P., Sica, A., and Balkwill, F. (2008). Cancer-related inflammation. Nature *454*, 436-444.
Marella, N. V., Seifert, B., Nagarajan, P., Sinha, S., and Berezney, R. (2009). Chromosomal rearrangements during human epidermal keratinocyte differentiation. J Cell Physiol *221*, 139-146.
Marzioni, D., Lorenzi, T., Mazzucchelli, R., Capparuccia, L., Morroni, M., Fiorini, R., Bracalenti, C., Catalano, A., David, G., Castellucci, M.*, et al.* (2009). Expression of basic fibroblast growth factor, its receptors and syndecans in bladder cancer. Int J Immunopathol Pharmacol *22*, 627-638.
McClintock, B. (1941). The Stability of Broken Ends of Chromosomes in Zea Mays. Genetics *26*, 234-282.
McClintock, B. (1942). The Fusion of Broken Ends of Chromosomes Following Nuclear Fusion. Proc Natl Acad Sci U S A *28*, 458-463.
McCormick, D. L., Phillips, J. M., Horn, T. L., Johnson, W. D., Steele, V. E., and Lubet, R. A. (2010). Overexpression of cyclooxygenase-2 in rat oral cancers and prevention of oral carcinogenesis in rats by selective and nonselective COX inhibitors. Cancer Prev Res (Phila Pa) *3*, 73-81.
McEachern, M. J., and Blackburn, E. H. (1995). Runaway telomere elongation caused by telomerase RNA gene mutations. Nature *376*, 403-409.
Meaburn, K. J., and Misteli, T. (2007). Cell biology: chromosome territories. Nature *445*, 379-781.
Meyer, N., and Penn, L. Z. (2008). Reflecting on 25 years with MYC. Nat Rev Cancer *8*, 976-990.
Misteli, T. (2001). The concept of self-organization in cellular architecture. J Cell Biol *155*, 181-185.
Misteli, T. (2005). Concepts in nuclear architecture. Bioessays *27*, 477-487.
Misteli, T. (2007). Beyond the sequence: cellular organization of genome function. Cell *128*, 787-800.
Molenaar, C., Wiesmeijer, K., Verwoerd, N. P., Khazen, S., Eils, R., Tanke, H. J., and Dirks, R. W. (2003). Visualizing telomere dynamics in living mammalian cells using PNA probes. Embo J *22*, 6631-6641.
Müller, H. (1938). The remaking of chromosomes. Collecting Net *13*, 181-198.
Murnane, J. P., and Sabatier, L. (2004). Chromosome rearrangements resulting from telomere dysfunction and their role in cancer. Bioessays *26*, 1164-1174.
Murnane, J. P., Sabatier, L., Marder, B. A., and Morgan, W. F. (1994). Telomere dynamics in an immortal human cell line. Embo J *13*, 4953-4962.
Nesbit, C. E., Tersak, J. M., and Prochownik, E. V. (1999). MYC oncogenes and human neoplastic disease. Oncogene *18*, 3004-3016.

Neuveut, C., Wei, Y., and Buendia, M. A. (2010). Mechanisms of HBV-related hepatocarcinogenesis. J Hepatol.
Nowell, P. C. (1976). The clonal evolution of tumor cell populations. Science *194*, 23-28.
Olovnikov, A. M. (1973). A theory of marginotomy. The incomplete copying of template margin in enzymic synthesis of polynucleotides and biological significance of the phenomenon. J Theor Biol *41*, 181-190.
Pampalona, J., Soler, D., Genesca, A., and Tusell, L. Whole chromosome loss is promoted by telomere dysfunction in primary cells. Genes Chromosomes Cancer *49*, 368-378.
Parada, L. A., McQueen, P. G., and Misteli, T. (2004). Tissue-specific spatial organization of genomes. Genome Biol *5*, R44.
Parada, L. A., McQueen, P. G., Munson, P. J., and Misteli, T. (2002). Conservation of relative chromosome positioning in normal and cancer cells. Curr Biol *12*, 1692-1697.
Pienta, K. J., Partin, A. W., and Coffey, D. S. (1989). Cancer as a disease of DNA organization and dynamic cell structure. Cancer Res *49*, 2525-2532.
Ploem, J. S. (1967). The use of a vertical illuminator with interchangeable dichroic mirrors for fluorescence microscopy with incidental light. Z Wiss Mikrosk *68*, 129-142.
Porichi, O., Nikolaidou, M. E., Apostolaki, A., Tserkezoglou, A., Arnogiannaki, N., Kassanos, D., Margaritis, L., and Panotopoulou, E. (2009). BCL-2, BAX and P53 expression profiles in endometrial carcinoma as studied by real-time PCR and immunohistochemistry. Anticancer Res *29*, 3977-3982.
Prochownik, E. V. (2008). c-Myc: linking transformation and genomic instability. Curr Mol Med *8*, 446-458.
Raz, V., Vermolen, B. J., Garini, Y., Onderwater, J. J., Mommaas-Kienhuis, M. A., Koster, A. J., Young, I. T., Tanke, H., and Dirks, R. W. (2008). The nuclear lamina promotes telomere aggregation and centromere peripheral localization during senescence of human mesenchymal stem cells. J Cell Sci *121*, 4018-4028.
Riley, T., Sontag, E., Chen, P., and Levine, A. (2008). Transcriptional control of human p53-regulated genes. Nat Rev Mol Cell Biol *9*, 402-412.
Rimawi, M. F., Shetty, P. B., Weiss, H. L., Schiff, R., Osborne, C. K., Chamness, G. C., and Elledge, R. M. (2010). Epidermal growth factor receptor expression in breast cancer association with biologic phenotype and clinical outcomes. Cancer *116*, 1234-1242.
Roix, J. J., McQueen, P. G., Munson, P. J., Parada, L. A., and Misteli, T. (2003). Spatial proximity of translocation-prone gene loci in human lymphomas. Nat Genet *34*, 287-291.
Ryott, M., Wangsa, D., Heselmeyer-Haddad, K., Lindholm, J., Elmberger, G., Auer, G., Avall Lundqvist, E., Ried, T., and Munck-Wikland, E. (2009). EGFR protein overexpression and gene copy number increases in oral tongue squamous cell carcinoma. Eur J Cancer *45*, 1700-1708.

Schaefer, L. H., Schuster, D., and Herz, H. (2001). Generalized approach for accelerated maximum likelihood based image restoration applied to three-dimensional fluorescence microscopy. J Microsc *204*, 99-107.
Schneider, R., and Grosschedl, R. (2007). Dynamics and interplay of nuclear architecture, genome organization, and gene expression. Genes Dev *21*, 3027-3043.
Skagias, L., Politi, E., Karameris, A., Sambaziotis, D., Archondakis, A., Vasou, O., Ntinis, A., Michalopoulou, F., Moreas, I., Koutselini, H., and Patsouris, E. (2009). Prognostic impact of HER2/neu protein in urothelial bladder cancer. Survival analysis of 80 cases and an overview of almost 20 years' research. J Buon *14*, 457-462.
Slamon, D. J., Godolphin, W., Jones, L. A., Holt, J. A., Wong, S. G., Keith, D. E., Levin, W. J., Stuart, S. G., Udove, J., Ullrich, A., and et al. (1989). Studies of the HER-2/neu proto-oncogene in human breast and ovarian cancer. Science *244*, 707-712.
Solovei, I., Kreysing, M., Lanctot, C., Kosem, S., Peichl, L., Cremer, T., Guck, J., and Joffe, B. (2009). Nuclear architecture of rod photoreceptor cells adapts to vision in mammalian evolution. Cell *137*, 356-368.
Spector, D. L. (2003). The dynamics of chromosome organization and gene regulation. Annu Rev Biochem *72*, 573-608.
Stein, G. S., Lian, J. B., Montecino, M., Stein, J. L., van Wijnen, A. J., Javed, A., Pratap, J., Choi, J., Zaidi, S. K., Gutierrez, S.*, et al.* (2003a). Nuclear microenvironments support physiological control of gene expression. Chromosome Res *11*, 527-536.
Stein, G. S., Zaidi, S. K., Braastad, C. D., Montecino, M., van Wijnen, A. J., Choi, J. Y., Stein, J. L., Lian, J. B., and Javed, A. (2003b). Functional architecture of the nucleus: organizing the regulatory machinery for gene expression, replication and repair. Trends Cell Biol *13*, 584-592.
Stewenius, Y., Gorunova, L., Jonson, T., Larsson, N., Hoglund, M., Mandahl, N., Mertens, F., Mitelman, F., and Gisselsson, D. (2005). Structural and numerical chromosome changes in colon cancer develop through telomere-mediated anaphase bridges, not through mitotic multipolarity. Proc Natl Acad Sci U S A *102*, 5541-5546.
Stokes, G. G. (1852). On the Change of Refrangibility of Light. Philosophical Transactions of the Royal Society of London, 463–562.
Stone, J., de Lange, T., Ramsay, G., Jakobovits, E., Bishop, J. M., Varmus, H., and Lee, W. (1987). Definition of regions in human c-myc that are involved in transformation and nuclear localization. Mol Cell Biol *7*, 1697-1709.
Sukenik-Halevy, R., Fejgin, M., Kidron, D., Goldberg-Bittman, L., Sharony, R., Biron-Shental, T., Kitay-Cohen, Y., and Amiel, A. (2009). Telomere aggregate formation in placenta specimens of pregnancies complicated with pre-eclampsia. Cancer Genet Cytogenet *195*, 27-30.
Szarvas, T., Becker, M., Vom Dorp, F., Gethmann, C., Totsch, M., Bankfalvi, A., Schmid, K. W., Romics, I., Rubben, H., and Ergun, S. (2010). Matrix

metalloproteinase-7 as a marker of metastasis and predictor of poor survival in bladder cancer. Cancer Sci.
Thiery, J. P. (2002). Epithelial-mesenchymal transitions in tumour progression. Nat Rev Cancer *2*, 442-454.
Tokutake, Y., Matsumoto, T., Watanabe, T., Maeda, S., Tahara, H., Sakamoto, S., Niida, H., Sugimoto, M., Ide, T., and Furuichi, Y. (1998). Extra-chromosomal telomere repeat DNA in telomerase-negative immortalized cell lines. Biochem Biophys Res Commun *247*, 765-772.
van Leeuwenhoek, A., Hoole, S. (1800). The select work of Antony van Leeuwenhoek: containing his microscopical discoveries in many of the works of nature, Vol 2: London: G. Sidney).
Vermolen, B. J., Garini, Y., Mai, S., Mougey, V., Fest, T., Chuang, T. C., Chuang, A. Y., Wark, L., and Young, I. T. (2005). Characterizing the three-dimensional organization of telomeres. Cytometry A *67*, 144-150.
Watson, J. D. (1972). Origin of concatemeric T7 DNA. Nat New Biol *239*, 197-201.
Weierich, C., Brero, A., Stein, S., von Hase, J., Cremer, C., Cremer, T., and Solovei, I. (2003). Three-dimensional arrangements of centromeres and telomeres in nuclei of human and murine lymphocytes. Chromosome Res *11*, 485-502.
Woodcock, C. L. (2006). Chromatin architecture. Curr Opin Struct Biol *16*, 213-220.
Wright, S. M., Woo, Y. H., Alley, T. L., Shirley, B. J., Akeson, E. C., Snow, K. J., Maas, S. A., Elwell, R. L., Foreman, O., and Mills, K. D. (2009). Complex oncogenic translocations with gene amplification are initiated by specific DNA breaks in lymphocytes. Cancer Res *69*, 4454-4460.
Yeager, T. R., Neumann, A. A., Englezou, A., Huschtscha, L. I., Noble, J. R., and Reddel, R. R. (1999). Telomerase-negative immortalized human cells contain a novel type of promyelocytic leukemia (PML) body. Cancer Res *59*, 4175-4179.
Yee, K. S., and Vousden, K. H. (2005). Complicating the complexity of p53. Carcinogenesis *26*, 1317-1322.
Zhang, D., Li, B., Shi, J., Zhao, L., Zhang, X., Wang, C., Hou, S., Qian, W., Kou, G., Wang, H., and Guo, Y. (2010). Suppression of Tumor Growth and Metastasis by Simultaneously Blocking Vascular Endothelial Growth Factor (VEGF)-A and VEGF-C with a Receptor-Immunoglobulin Fusion Protein. Cancer Res.
Zhang, M., Zhang, P., Zhang, C., Sun, J., Wang, L., Li, J., Tian, Z., and Chen, W. (2009). Prognostic significance of Bcl-2 and Bax protein expression in the patients with oral squamous cell carcinoma. J Oral Pathol Med *38*, 307-313.
Zheng, H., Ying, H., Yan, H., Kimmelman, A. C., Hiller, D. J., Chen, A. J., Perry, S. R., Tonon, G., Chu, G. C., Ding, Z.*, et al.* (2008). Pten and p53 converge on c-Myc to control differentiation, self-renewal, and transformation of normal and neoplastic stem cells in glioblastoma. Cold Spring Harb Symp Quant Biol *73*, 427-437.
Zullo, A., Hassan, C., Cristofari, F., Andriani, A., De Francesco, V., Ierardi, E., Tomao, S., Stolte, M., Morini, S., and Vaira, D. (2010). Effects of Helicobacter

pylori eradication on early stage gastric mucosa-associated lymphoid tissue lymphoma. Clin Gastroenterol Hepatol *8*, 105-110.